PEOPLE'S DEMOCRATIC REPUBLIC OF ALGERIA

MINISTRY OF HIGHER EDUCATION AND SCIENTIFIC RESEARCH

University Amar Telidji- Laghouat

FACULTY: Technology

DEPARTEMENT: Electrotechnic

MASTER MEMOIR

Presented by: MIHOUBI Omar Elfarouk

BEN DJEMAI Hadj Belkacem

DOMAIN: Sciences and Technology

FIELD: Electrical Engineering

OPTION: Electrical Power System

Theme

Automatic Generation Control in Low Inertia Power System

Defense jury:

full name	Grade	Quality
CHETTIH Saliha	Prof	Jury President
OUBBATI Youcef	M.C.B	Examiner
ARIF Salem	Prof	Supervisor
ABBOU Hossam Eddine	PhD Student	Co-Supervisor

Academic Year: 2021-2022

ملخص : قد ينخفض القصور الذاتي للنظام الكلي في نظام طاقة مترابط بشكل كبير نتيجة للنمو السريع في استخدام مصادر الطاقة المتجددة القائمة على محول الطاقة (RESs), زيادة حساسية نظام الطاقة المترابط تجاه عدم استقرار النظام. تقدم هذه المذكرة تطبيقا للتحكم الافتراضي في القصور الذاتي (VIC) في مراقب الانتاج الاوتوماتيكي (AGC) لتحسين استقرار التردد لنظام الطاقة المترابط بمستويات اختراق عالية من(RESs) (نظام الطاقة مع القصور الذاتي المنخفض). في هذه الدراسة، MATLAB/Simulink® يستخدم لنمذجة النظام ومحاكاة النتائج. يتم استخدام نظام اختبار متعدد المناطق بمستوى اختراق RESs عالي لظروف مختلفة للتحقق من كفاءة مفهوم التحكم الافتراضي في القصور الذاتي في تعزيز الاستقرار. أجهزة التحكم التقليدية ، مثل وحدات التحكم (PID), تم اقتراحه لمحاكاة القصور الذاتي لنظام الطاقة باستخدام (VIC).

الكلمات المفتاحية : مراقب الانتاج الاوتوماتيكي (AGC) ، القصور الذاتي المنخفض ، نظام الطاقة المترابط ، RES، VIC ، وحدات التحكم.

Résumé : L'inertie globale du système dans un Système de Puissance interconnecté peut être considérablement réduite en raison d'une croissance rapide de l'utilisation des Sources D'énergie Renouvelables (RESs) basées sur des convertisseurs de puissance, augmentant la sensibilité du Système de Puissance interconnecté à l'instabilité du système. Cette thèse propose une application du Virtual Inertie Control (VIC) dans le Contrôle de Génération Automatique (AGC) pour améliorer la stabilité de fréquence du Système de Puissance interconnecté avec des niveaux de pénétration élevés des RESs (Système de Puissance à faible inertie). Dans cette étude, MATLAB/Simulink® est utilisé pour modéliser le système et simuler les résultats. Un système de test multi-zones avec un niveau de pénétration élevé des RESs pour différentes circonstances est utilisé pour vérifier l'efficacité du concept de Contrôle d'Inertie Virtuelle sur l'amélioration de la stabilité. Contrôleurs conventionnels, tels que les contrôleurs Proportionnels-Intégraux -Dérivés (PID), ont été proposés pour émuler l'inertie du Système de Puissance à l'aide de méthodes VIC.

Mots clés : Contrôle de Génération Automatique (AGC), Faible Inertie, Système de Puissance Interconnecté, RESs, VIC, Contrôleurs.

Abstract: The overall system inertia in an interconnected power system may be considerably reduced as a result of a rapid growth in the use of power converter-based Renewable Energy Sources (RESs), increasing the interconnected power system's sensitivity to system instability. This thesis offers an application of Virtual Inertia Control (VIC) in the Automatic Generation Control (AGC) to improve frequency stability of the interconnected power system with high penetration levels of RESs (power system with low-inertia). In this study, MATLAB/Simulink® is used to model the system and simulate the results. A multi-area test system with high RESs penetration level for different circumstances is used to verify the efficiency of the Virtual Inertia Control concept on stability enhancement. Conventional controllers, such as Proportional-Integral-Derivative (PID) controllers, have been proposed to emulate power system inertia using VIC methods.

Keywords: Automatic Generation Control (AGC), Low Inertia, Interconnected Power System, RES, VIC, Controllers.

Dedication

*First, before anything, thanks to '**Allah**' who guides, helps and gives me the capacity to do this work.*

To my dear parents whom I owe my success. They always encouraged a love of learning in and expected the best of me

*I would like to express my infinite gratitude and respect to my supervisor **Pr. ARIF Salem** and **Mr. ABBOU Hossam Eddine Aymane** for they constant help, precious suggestions and valuable advices.*

To all my extended family

To all my friends and teachers at the University of Laghouat

To all who were there for me, thank you for your help and encouragement

Thank you all for you help.

OMAR

Dedication

To the dearest people to my hearts

Starting by my parents

Moving to my sisters and brothers

To all my family members

To all my teachers

And a special thank to all people who have stood by us in our hard moments.

Belkacem

Acknowledgment

All thanks to, our sincere appreciation is given to our supervisors**, Pr. ARIF Salem** and **Mr. ABBOU Hossam Eddine Aymane**, for their amazing guidance, support and wise words of encouragement from the very beginning and throughout the development of the thesis.

In particular, their gentle and compassionate approach of supervision crucially helped to render the thesis journey a pleasant experience. Without them, this research would not have been possible and we thank also the members of the jury for reading and evaluating our thesis.

We would take this excellent opportunity to express our appreciation to all the teachers who taught us and would also like to thank all the people who have contributed significantly to the achievement of this work and its success.

We are truly grateful.

Contents

List of Figures

List of Tables

Nomenclature

Symbols

A	Coefficient vector
A_{PV}	The measured area of PV array (m^2)
As	The swept area of blade (m^2)
a	Linearly decreased
B	Frequency bias coefficient
C	Coefficient vector
C_p	The power co-efficient which is a function of tip speed ratio (λ)
D	Damping coefficient
D'	The distance between the whale and prey
$E_{kinetic}$	Kinetic energy
H	The inertia constant
J	The moment of the system inertia (kgm^2)
K	The area bias
K_I	Gain of the integral action
K_D	Gain of the proportional action
K_P	Gain of the proportional action
K_{VI}	Gain of the virtual inertia
R	Speed governor (Hz/p.u MW)
S	The system rated power (VA)

T_a	The ambient temperature (C°)
T_D	The derivative time constant (s)
T_g	Steam turbine speed /governor time constant (s)
T_I	The integral time constant (s)
T_{PV}	The gain constant and the time constant (in s) of the SPG
T_T	Re-heater time constant (s)
T_{VI}	The virtual inertia time constant
T_{WT}	The gain constant and the time constant (in s) of the WPG
X	The whale's position vector
$Xrand$	Random position vector
$X*$	The prey position vector
Δf	Frequency deviation (Hz)
$\Delta Ptei$	Tie line power deviation (p.u)
ΔPm	Mechanical power deviation (p.u)
ΔPv	The valve position change (p.u)
ΔPe	Electrical power deviation (p.u)
ΔPg	Generation power deviation (p.u)
ΔPl	Load variation (p.u)
$\Delta P_{inertia}$	Inertia power deviation (p.u)
ω	The rotor speed (rad/s),
ρ	The air density (kg/m^3)
$v\omega$	The velocity of the wind

η	The conversion efficiency (%) of the PV array
φ	The solar irradiance (W/m^2)

Acronyms and abbreviations

ACE	Area Control Error
AGC	Automatic Generation Control
IAE	Integral of The Absolute Error
ISE	Integral of The Squared Error
ITAE	Integral of Time Multiplied by The Absolute Error
ITSE	Integral of Time Multiplied by The Squared Error
LFC	Load Frequency Control
PID	Proportional Integral Derivative
PO	Peak Overshoot
PU	Peak Undershoot
WPG	Wind Power Generation
SPG	Solar Power Generation
RESs	Renewable Energy Sources
GRC	Generation Rate Constraint
GDB	Governor Dead-Band
VIC	Virtual Inertia Control
WOA	Whale Optimization Algorithm
ROCOF	The Rate of Change of Frequency
VISMA	Virtual Synchronous Machine

ESS	Energy Storage System
IEPE	Institute of Electrical Power Engineering
KHI	Kawasaki Heavy Industries
SPC	Synchronous Power Controller
VSG	Virtual Synchronous Generators
VOC	Virtual Oscillator Control
VSYNC	Vertical Synchronization

GENERAL INTRODUCTION

General Introduction

Problematic

In power systems, frequency stability is significant in the stable and safe operation of power systems, reflecting the fundamental position of power systems in generation and demand. An imbalance could lead to continual deviation of the system frequency [1]. The load always changes a lot during a daily cycle, this needs a balance of power, and generators need to produce more or less power to keep up with the demand. For that Automatic Generation Control (AGC) is used, which has been an important feature of electrical power system for the last decades that manages to supply reliable and economical electricity for modern power consumers. Therefore, the primary responsibility of AGC is to keep the system generations in sync with the load demand, as well as to keep the system frequency and the exchange of power between control regions (tie-line power) within the set nominal value [2]. The role of Automatic Generation Control (AGC) is [3]:

- To restore system frequency deviation to within predefined limits around nominal frequency
- To maintain the correct value of interchanged power between control areas.
- To preserve each unit's generation at the most economic value.

Generally, there are four control loops in the AGC problem. We can site the well treated ones:

- Primary Control Loop (PCL)

The function of PCL is to re-establish a balance between generation and load at frequency different from its nominal value.

- Secondary Control Loop (SCL)

The function of SCL called Load Frequency Control (LFC) is to restore power cross-border exchanges to their set-point values and to restore the System Frequency to its set-point value at the same time[3].

Recently, the increase of Renewable Energy Sources (RESs) utilization in power systems has turned out to be inevitable. However, the intermittent energy generations from the RESs cause fluctuation problems of power system frequency and voltage due to their dependency on weather conditions. These problems may lead to limiting the high penetration levels of RESs in power systems [4]. The integration of Renewable Energy Sources (RES) such as photovoltaic (PV) and wind farms. This fact may have a negative influence on power system performance, particularly inertia response and damping qualities [5].

General Introduction

A Brief Survey on The AGC Problem

Apart from advancements in AGC design techniques, additional developments over the last two decades have included the advent of Renewable Energy Sources (RES) and deregulation of power sectors, providing new problems for power engineers to deal with these changes [6].

With the increasing impact of low inertia due to the high penetration of RESs, virtual synchronous generator (VSG) technology has been proposed to improve the stability of the inverter-interfaced RESs by providing "virtual inertia"[7].

For more realistic study, several non-linear constraints such as Governor Dead Band (GDB), Generation Rate constraint (GRC), Dynamic Boiler (DB), Time Delay (TD) have been introduced [8,9].

Many control approaches have been suggested for AGC in interconnected power systems such as classical control approaches focus on designing Proportional-Integral-Derivative (PID) [10,11].

Objectives of This Memoir

The main objectives of this memoir are presented as follow:

- To develop the AGC problem taking in consideration the effect RESs end different constraints such as GDB, GRC in the performance of the system;
- To try and implement other control technics such as Virtual Inertia Control (VIC), and see if it can improve the performance of the system;
- To well understand the effect of inertia in the system

Memoir Outlines

This memoir is divided into the following three main chapters:

Chapter 1

- Provides some fundamental about the AGC control loops and some models. Then, we will see some types of constraints for more realistic study. Finally, a description about the detailed linearized models of Wind Power Generation (WPG) unit and Solar Power Generation (SPG) unit.

Chapter 2

- Explains what is inertia and its effect, it provides some solution then gives the concept of Virtual Inertia Control VIC. Then, a brief description of PID controller used in our study is

presented. Finally, generality about meta-heuristics and the description of a new optimization algorithm called Whale Optimization Algorithm (WOA) are exposed.

Chapter 3

- Provides the investigations which are carried out in two-area thermal power plants with appropriate nonlinearities such as GRC and GDB integrating high penetration of RESs in each area. After that, we will see the effect of inertia on the system without VIC. after that, the system will be subjected to an abrupt change in load to test the effectiveness of implementing VIC. in addition, this chapter goes through another inertia effect again but with the presence of VIC this time. Lastly, to confirm the robustness of the proposed control technic, the system goes under random RESs and load disturbances. All the optimal control settings of PID and VIC are given in this chapter optimized using WOA.

CHAPTER I:
AGC With RESs

I.1. Introduction

Automatic Generation Control (AGC) is one of the important control problems in electric power system design and operation, it is becoming more important nowadays as Renewable Energy Sources (RESs) such as wind and solar farms proliferate. The power fluctuation induced by a large penetration of wind and solar farms contributes to power imbalance and frequency variation in a negative way [12]. In This chapter, we're going to talk about the various AGC control loops and some models are given. Then, a number of non-linear constraints are presented and discussed. Finally, a describetion about the detailed linearized models of Wind Power Generation (WPG) unit and Solar Power Generation (SPG) unit is given.

I.2. Power Generating Units

The mathematical modeling of the system is the initial step in the study and design of a control system. The transfer function method and the state variable approach are the two most common methods. The state variable method may be applied to represent both linear and nonlinear systems. The system must first be linearized before using the transfer function and linear state equations. The mathematical equations representing the system are linearized using appropriate assumptions and approximations, and a transfer function model for the following components is obtained [13].

I.2.1. Generator and Load Models

A power system's loads are typically made up of a variety of electrical devices. For resistive loads such as lighting and heating, electrical power is not affected by frequency. Motor loads are sensitive to changes in frequency [13]. The overall frequency dependent characteristic of a composite load is approximated by equation (I.1):

$$\Delta \mathrm{Pe} = \Delta \mathrm{PL} - \mathrm{D}\Delta\omega \qquad \text{(I.1)}$$

For a 1% change in frequency, the damping coefficient is commonly stated as a percent change in load [14].

In this section, a simplified frequency response model for the described schematic block diagram in Fig. I.1 with one generator unit is described. The overall generator–load dynamic relationship between the incremental mismatch power ($\Delta P\mathrm{m} - \Delta P\mathrm{L}$) and the generator's rotor speed output ($\Delta\omega$) (frequency of the power systems) can be expressed as:

$$\Delta Pm\,(t) - \Delta Pe\,(t) = 2H\,\frac{d\Delta\omega\,(t)}{dt} \quad (I.2)$$

$$\Delta Pm\,(t) - \Delta PL\,(t) = 2H\,\frac{d\Delta\omega\,(t)}{dt} + D\Delta\omega\,(t) \quad (I.3)$$

Using the Laplace transform, (I.3) can be written as:

$$\Delta Pm\,(s) - \Delta PL\,(s) = 2H\,s\Delta\omega\,(s) + D\Delta\omega\,(s) \quad (I.4)$$

$$\Delta\omega\,(s) = \frac{1}{2Hs + D}\,(\,\Delta Pm\,(s) - \Delta PL\,(s)\,) \quad (I.5)$$

Equation (I.5) can be represented in a block diagram as in Fig. I.1 [14]

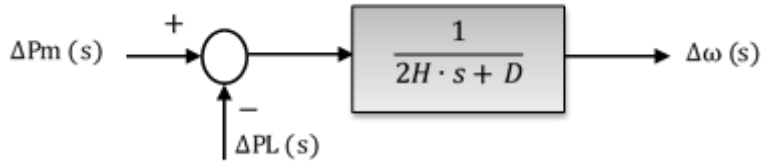

Fig. I.1: Generator and load block diagram

I.2.2. Turbine and Governor Models

The prime mover is the main source of mechanical power, such as hydraulic turbines at waterfalls, steam turbines whose energy comes from the burning of coal, gas, nuclear fuel, and gas turbines. The model of the turbines relates change in mechanical power output ΔPm to changes in steam valve position ΔPv. Different types of turbines vary widely in characteristics [15].

a. Steam Turbine Model

- The Non-Reheat Turbines

. The simplest prime mover model for non-reheat steam turbine can be approximated with a single time constant T_T [15] .non-reheat turbine transfer feature can be defined as :

$$G_T(s) = \frac{\Delta Pm(s)}{\Delta Pv(s)} = \frac{1}{1 + T_T s} \quad (I.6)$$

The block diagram for a simple non-reheat turbine is shown in Fig. I.2 below.

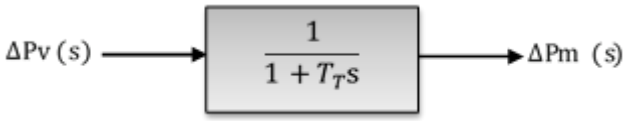

Fig. I.2: Block diagram for a simple non-reheat steam turbine

b. Governor

The real power in a power system is controlled by regulating the driving torques of the individual turbines (steam or hydro) of the system.

By controlling the position measured by the coordinate X_E, of the governor controlled valves (or gates, in the case of a hydro-turbine), we can exert control over the flow of high-pressure steam (or water) through the turbine. Very large mechanical forces are needed to position the main valve (or gate) against the high steam (or hydro) pressure and these forces are obtained via several stages of hydraulic amplifiers. In our simplified version, we show only stages: the input to this amplifier is the position X_D; the output of the pilot valve is the position X_E of the main piston. Because the high differential force on the pilot valve, the force amplification is very great. The position of the pilot valve can be affected via the linkage system in three ways:

- Directly, by moving the linkage point A by "raise" or "lower" commands of the speed changer.
- Indirectly, via feedback, due to position changes of the main piston.
- Indirectly, via feedback, due to position changes linkage point B resulting from speed changes [16].

The first governors were the watt governors that sensed the speed by spinning fly balls and produced mechanical motion in response to changes in temperature. Most modern governors however use electronic devices to detect changes in speed. Fig. I.3 schematically shows the essential elements of a standard watt governor composed of the following major sections [13]:

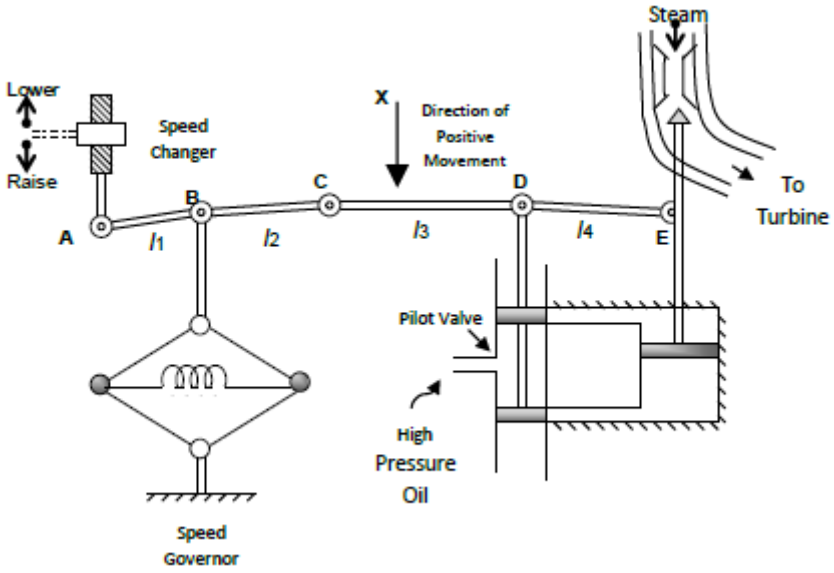

Fig. I.3: Speed governing system.

By adjusting this set point, a desired load dispatch can be scheduled at nominal frequency.

For a stable operation, the governors are designed to permit the speed to drop as the load is increased. Fig I.4 shows the steady-state features of such governor:

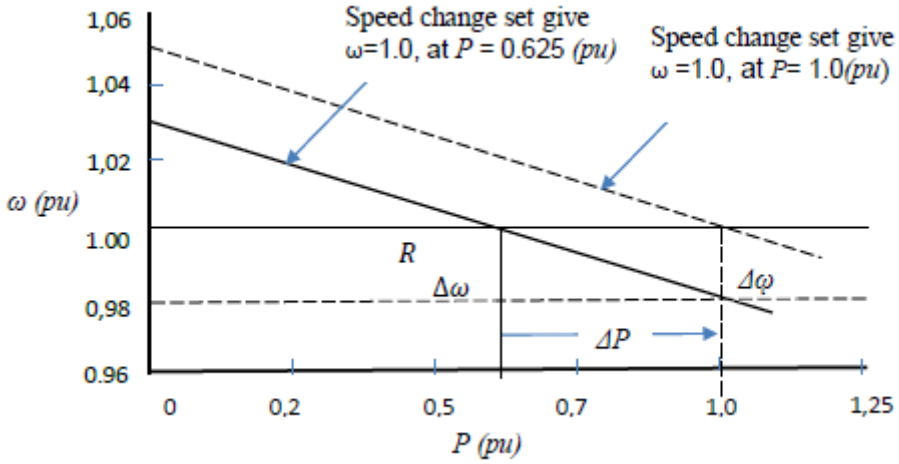

Fig. I.4: Governor steady-state speed characteristics

The slope of the curve represents the speed regulation R. The mechanism of the speed governor acts as a comparator whose output ΔP_g is the difference between the power ΔP_{ref} and the power $\frac{1}{R}\Delta\omega$ as speed characteristics provided by the governor [13].

$$\Delta P_g = \Delta P_{ref} - \frac{1}{R}\Delta\omega \quad \text{(I.7)}$$

Or in s-domain:

$$\Delta P_g(s) = \Delta P_{ref}(s) - \frac{1}{R}\Delta\omega(s) \quad \text{(I.8)}$$

Assume linear time constant, the command ΔPg is converted into the steam valve position command ΔP_V and we considering a simple time constant Tg, get the relation in s-domain.

$$\Delta P_V(s) = \Delta P_g(s) \frac{1}{1+T_g s} \quad \text{(I.9)}$$

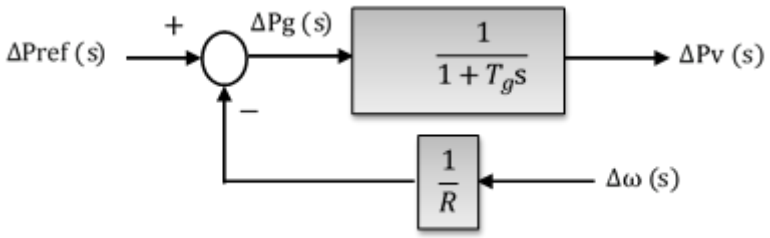

Fig. I.5: Block diagram representation of speed governing system for steam turbine

I.3. Power System AGC Models

For the power system configuration, most of the research relies on linearized models of single-area and multi-area power systems. This section explains the different methods of frequency control in major power system models.

I.3.1. AGC in Single Area

With the primary LFC loop, a change in the system load will result in a steady state frequency deviation, depending on the governor speed regulation. In order to reduce the frequency deviation to zero, we must provide a rest action. This rest action can be achieved by introducing an integral controller to act on the load reference setting to change the speed set point. The integral controller increases the system type by one which forces the final frequency deviation to zero. The integral controller gain K must be adjusted for a satisfactory transient response [15].

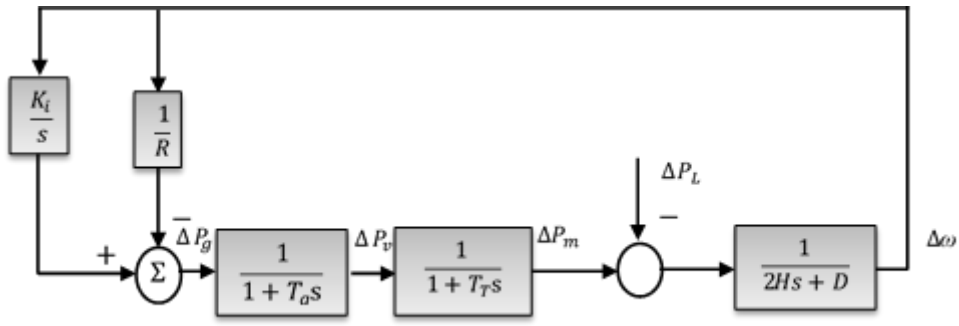

Fig. I.6: AGC for an isolated power system with secondary control.

I.3.2. AGC in Multi Area System

a) Two Area System With Primary Control

Consider two areas represented by an equivalent generating unit interconnected by a lossless tie line with X_{tie} reactance. Each region is represented behind an equivalent reactance by a voltage source as shown in Fig. I.7 [16].

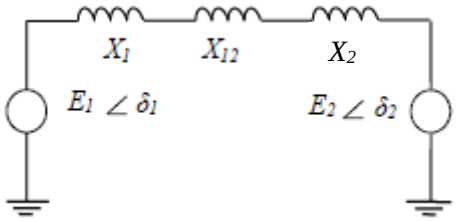

Fig. I.7: Equivalent network for two area power system

The real power transferred over the tie line is given during normal operation by:

$$P_{12}=\frac{|E1||E2|}{X12}\sin\delta 12 \qquad \text{(I.10)}$$

Where: $X_{12} = X_1 + X_{tie} + X_2$, and $\delta_{12} = \delta_1 - \delta_2$.

The tie line power deviation then takes on the form:

$$P_{12} = \quad P_2\,(\Delta\delta_1 - \Delta\delta_2) \qquad \text{(I.11)}$$

The tie line power flow appears to increase the load in one area and decrease the load in the other, depending on the direction of the flow. The direction of the current is dictated by the difference in the angle of phase; if $\Delta\delta 1 > \Delta\delta_2$, the power flows from area 1 to area 2 [13].

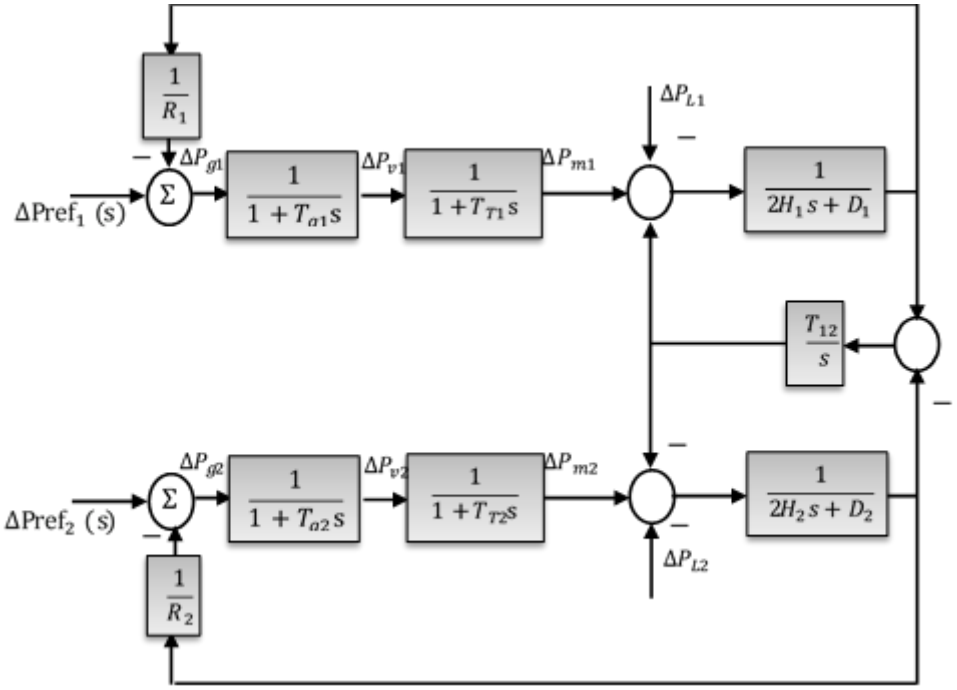

Fig. I.8: Two area system with primary LFC loop

b) Two Area System With Secondary Control

The power system operated normally, allowing the areas' demands to be satisfied at nominal frequency, for normal mode, a simple control strategy is [13]:

- Keeping the frequency at its nominal value;
- Maintaining the tie-line flow on schedule;
- Each zone will absorb its own charges.

In a two-area system, each area tends to minimize its area control error (ACE) to zero, which is given by this equation:

$$\text{ACEi} = \sum_{j=1}^{n} \Delta Pij + Ki\,\Delta\omega \qquad \text{(I.12)}$$

Where Ki is the area bias determines the amount of interaction during a disturbance in the neighboring areas. The satisfactory performance is achieved when Ki is selected equal to the frequency bias factor of that area, the ACEs for two areas are [13]:

$$\text{ACE}_1 = \Delta P_{12} + B_1 \Delta\omega_1 \qquad \text{(I.13)}$$

$$ACE_2 = \Delta P_{21} + B_2 \Delta\omega_2 \quad \text{(I.14)}$$

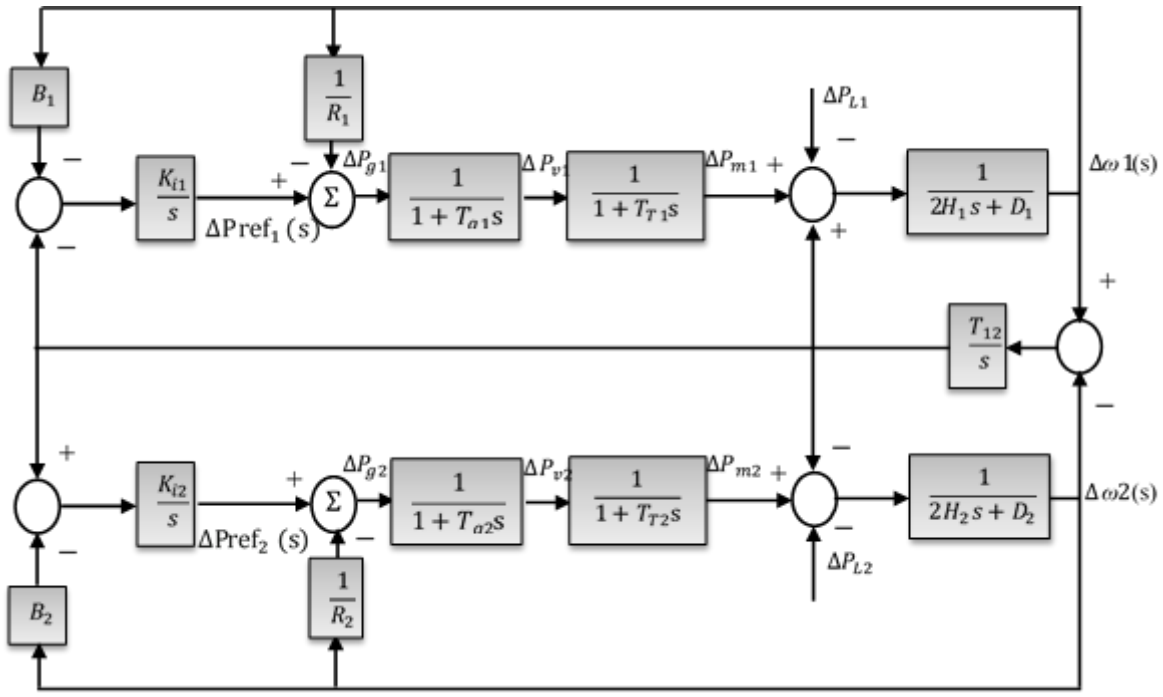

Fig. I.9: Block diagram of a basic AGC for two area system

I.4. Physical Constraints

To achieve more realistic results, nonlinear constraints such as GDB and GRC should be used

I.4.1. Generation Rate Constraint

An important constraint in the power system AGC is a limitation on the variation rate of mechanical movement which is known as generation rate constraint (GRC) [17]. In the block diagram of Fig. I.10:

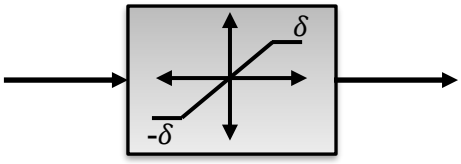

Fig. I.10: Non-linear turbine model with GRC

The rate of change in the power output of generating units utilized for AGC must be adequate for the AGC's overall purposes. This is expressed as a percentage of the control generator's rated output per unit of time. Generation units have varied rates based on their technology and type. Diesel engines, industrial GT, combined cycle GT, steam turbine plants, and nuclear power plants have typical ramp rates (as a percentage of capacity) are 40%/min, 20%/min, 5% to 10%/min, 1% to 5%/min, and 1% to

5%/min, respectively. In hard-coal and lignite-fired power plants, this rate is 2 to 4% per minute and 1 to 2% per minute, respectively [18].

I.4.2. Speed Governor Dead-Band

An important physical constraint is defined as the total magnitude of a sustained speed change, within which there is no resulting change in valve position. The limiting value of dead band is specified as 0.06% (0.036Hz) [19]. The speed governor dead band has a significant effect on the performance of the governors and it has a destabilizing effect on the transient performance of the system. For a wide dead-band, the AGC performance may be significantly degraded. The impact of the dead-band governor on the performance of the AGC is to increase the apparent steady state control of frequency [18].

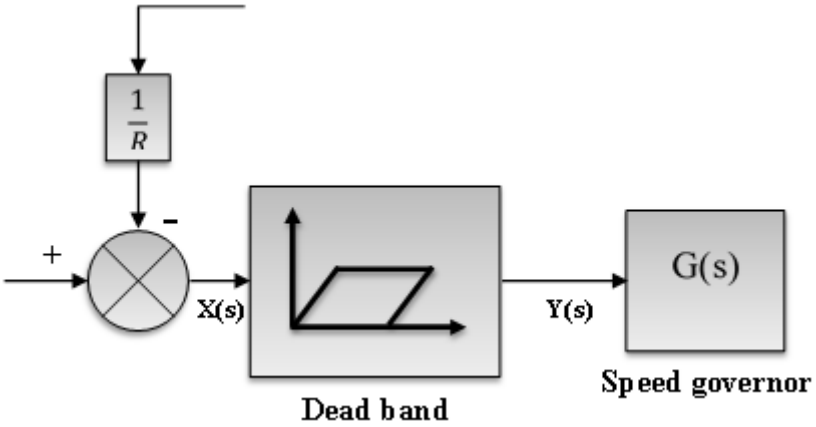

Fig. I.11: Block Diagram model of speed governor dead-band

I.5. AGC and Renewable Energy Options

The power system is currently undergoing fundamental changes in its structure. These developments are linked not only to the problem of deregulation and the implementation of competitive policies, but also to the adoption of new forms of power generation, new technology, and fast rising volumes of Renewable Energy Sources (RESs). The growing need for electrical energy, along with finite fossil fuel supplies and growing environmental concerns, necessitates rapid progress in the field of Renewable Energy Sources (RESs). Renewable energy is derived from natural sources such as the sun, wind, hydropower, biomass, geothermal, and oceans. Because of these developments, new AGC methods in contemporary power systems are required.

According to recent research, the effects of renewable integration on system frequency and power fluctuation are nonzero and become more significant as penetration sizes increase. Variability and uncertainty are two fundamental characteristics of variable RESs that have a significant influence

on bulk power system planning and operations. The main difficulties are caused by the variability and limited predictability of power from renewable sources such as wind, solar, and waves [18].

I.5.1. RESs Effect in Power System

The RESs affect the dynamic behaviour of the power system in a way that might be different from conventional generators. Conventional power plants mainly use synchronous generators that are able to continue operation during significant transient faults. If a large amount of wind or solar generation is tripped because of a fault, the negative effect of that fault on power system control and operation, including frequency control issue, could be magnified. High renewable energy penetration in power systems may increase uncertainties during abnormal operation and introduces several technical implications and opens important questions, as to whether the traditional power system control approaches to operation in the new environment are still adequate.

Integration of RESs into power system grids have impacts on optimum power flow, power quality, voltage and frequency control, system economics and load dispatch. Regarding the nature of RESs power variation, the impact on the frequency regulation issue has attracted increasing research interest, during the last decade. Significant interconnection frequency deviations can cause under/over frequency relaying and disconnect some loads and generations. Under unfavourable conditions, this may result in a cascading failure and system collapse [20].

I.5.2. RESs Models

In this model, automatic generation control (AGC) of a two-area power system with two different Renewbles Energy Sources. area-1 is integrated with SPG, area-2 is integrated with WPG.

a. Modeling of WPG

WPG is also gaining more interest as an alternative energy source. After solar, it is more effective and available energy producer. In the recent days many countries choose WPG as a promising alternative energy producer. In case of WPG, The wind turbine exploits the kinetic energy of the wind and converts it into mechanical power output (Pwt). The Pwt from the wind turbine is transferred to rotor of the generator to produce electrical power (Pwtg) via turbine-generator shaft. The governing equations representing mechanical power output from the wind turbine may be given by [21]:

$$P_{WT} = \frac{1}{2}\rho A_s C_p (v_w)^3 \qquad \text{(I.15)}$$

Where ρ is the air density (kg/m^3); As the swept area of blade (m^2), v_w is the velocity of the wind and C_p is the power co-efficient which is a function of tip speed ratio (λ) and blade pitch angle (β) [22]. WPG is a non-linear system. However, in the present work, simple linearized model of the WPG is considered and presented as the first-order lag transfer function model ($G_{WPG}(s)$) as shown in:

$$G_{WPG} = \frac{\Delta P_W}{\Delta P_{Wind}} = \frac{1}{1 + sT_{WT}} \quad \text{(I.16)}$$

Where T_{WT} : The gain constant and the time constant (s) of the WPG, respectively. P_W is the power output from WPG (in p.u.) and the symbol Δ represents the deviation in the associated parameter. In the present work, a practical wind farm model is used which is realized by means of white noise block with a low pass filte [23].

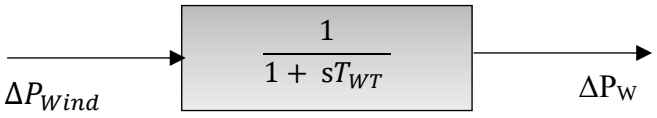

Fig. I. 12: Linearized model of WPG

b. Modeling of SPG

In SPG is one of the promising Renewable Energy Sources. As it is one of the alternative energy sources which produces CO_2 free power, flexible in nature and simple in use, in recent days it draws a huge interest to researchers and industrialists. One of the major constraints is SPG is dependent on solar irradiance (φ) in a constant temperature. When it works interconnected manner with thermal generation, then extra advantages in power balancing is observed [21]. In spite of high capital investment and poor conversion efficiency, SPGs have been found as the best and viable alternative options to bridge the gap between supply and demand of electrical energy. Moreover, a SPG (a) requires less maintenance, (b) has no moving parts, (c) emits no noise and (d) offers environment friendly energy conversion process [23]. The fundamental governing equation relating electrical power output (P_{SPG}) from a SPG system is given by:

$$P_{SPG} = \eta \varphi A_{PV} \{1 - 0.005 (T_a + 25)\} \quad \text{(I.17)}$$

Where η is the conversion efficiency (%) of the PV array, φ is the solar irradiance (W/m^2), A_{PV} is the measured area of PV array (m^2) and T_a is the ambient temperature (C°). In the present work, linearized

mathematical model of the SPG is incorporated and represented as the first-order lag transfer function model (G_{SPG} (s)) as shown in :

$$G_{SPG} = \frac{\Delta P_S}{\Delta P_{solar}} = \frac{1}{1 + sT_{PV}} \quad \text{(I.18)}$$

Where T_{PV}: The gain constant and the time constant (s) of the SPG, respectively.

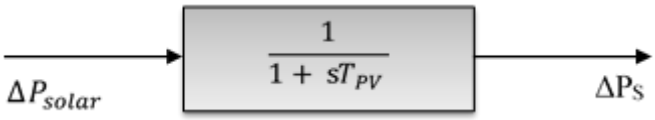

Fig. I.13: Linearized model of SPG

I.6. AGC with RESs Model

In this section, we are going to represent AGC two-area interconnected thermal power system with the presence of RESs (Solar and Wind power generations). Each area composed by speed governing system, turbine, generator, GDB and GRC

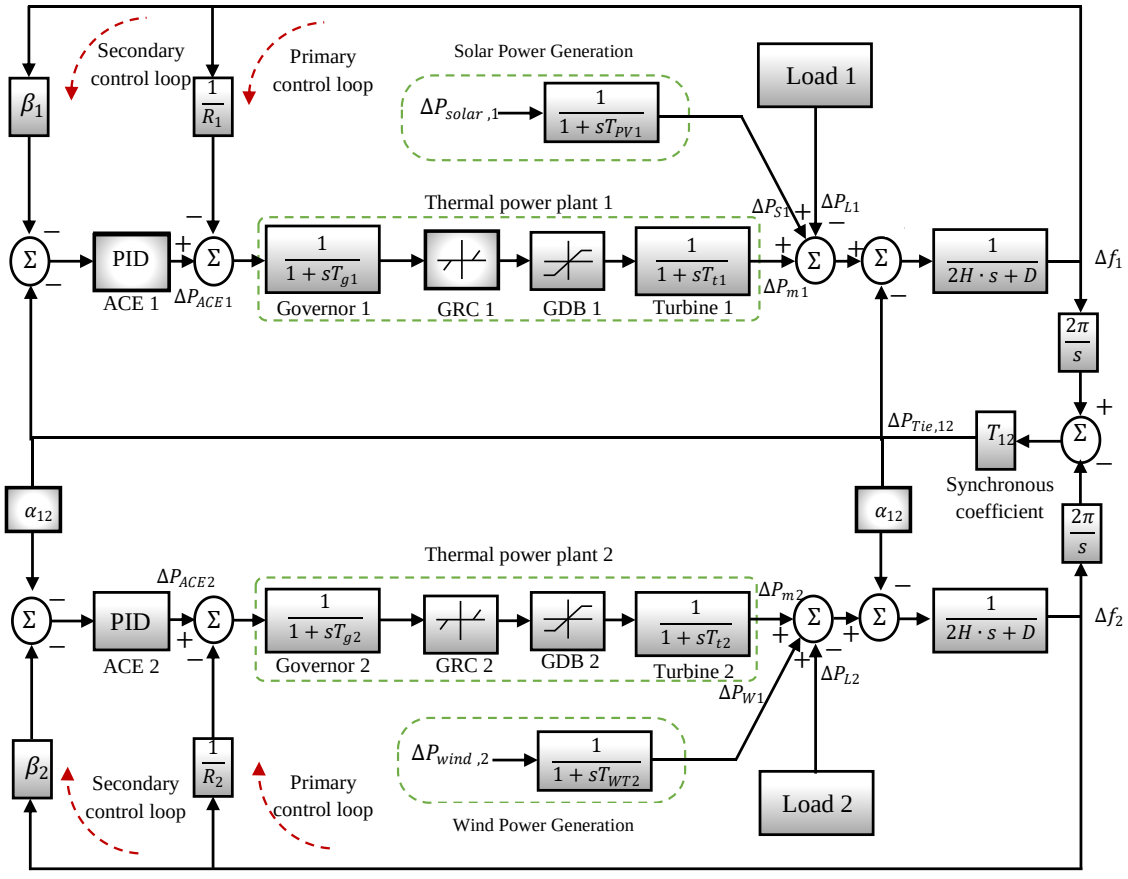

Fig. I.14: (AGC) of a two-area power system with two different Renewbles Energy Sources

I.7. Conclusion

This first part of this memoir includes a brief description of automatic generation control and its importance. Firstly, we have exposed the designing and modeling of the system power single and multi-areas for use in simulation. Also we've seen some types of constraints for more realistic study. Finally, we've seen the effect of the RESs in the power system and some RESs models.

CHAPTER II:

Low Inertia, PID and Optimization

II.1. Introduction

The integration of RESs in the power system is increasing rapidly all over the world. RESs is based on fast-response inverters, which decreases power system inertia and brings challenges to the stable operation. In this chapter, we're going to talk about the inertia definition, effect and control. After that, we will present briefly the PID regulator, with its optimization parameters. And finally, we will expose briefly a generality about meta-heuristics plus the description of this new optimization algorithm called Whale Optimization Algorithm (WOA).

II.2. What is Inertia?

Power system inertia is related to the stored energy in the rotating masses connected to the power system. It can also be defined as the period of time in which the stored energy in the rotating masses could be used to supply the total rated power. This energy is one of the basic parameters of the power system. For an individual generator, it is defined by the moment of inertia of the rotating mass, J, and the rotational speed. It is well known from basic physics that the moment of inertia of a rotating mass can be calculated from the ratio of the stored kinetic energy and its rated speed squared. Because the rotational speed of the rotating mass of a generator continuously changes around the nominal speed, ωr, it is assumed that it always rotates with nominal (synchronous) speed [24]. This assumption allows inertia to be redefined with the inertia constant, H, given by :

$$E_{kinetic} = \frac{1}{2} J\, \omega_n^2 \tag{II.1}$$

$$T_m - T_e = \frac{P_m}{\omega} - \frac{P_e}{\omega} = J\frac{d\omega}{dt} \tag{II.2}$$

$$H = \frac{E_{kinetic}}{S} \tag{II.3}$$

Where J denotes the moment of the system inertia (kgm^2), ω the rotor speed (rad/s), T_e and T_m represent the electrical and mechanical torque respectively. P_e and P_m represent the electrical and mechanical power respectively, and S is the system rated power (VA).

This way, when the inertia constant of each generator is normalized by the same rated power, the total inertia constant is obtained as a sum of each individual constants. The impact of inertia on frequency behaviour is expressed with a spring. Greater stiffness of the spring denotes higher inertia and vice versa [24].

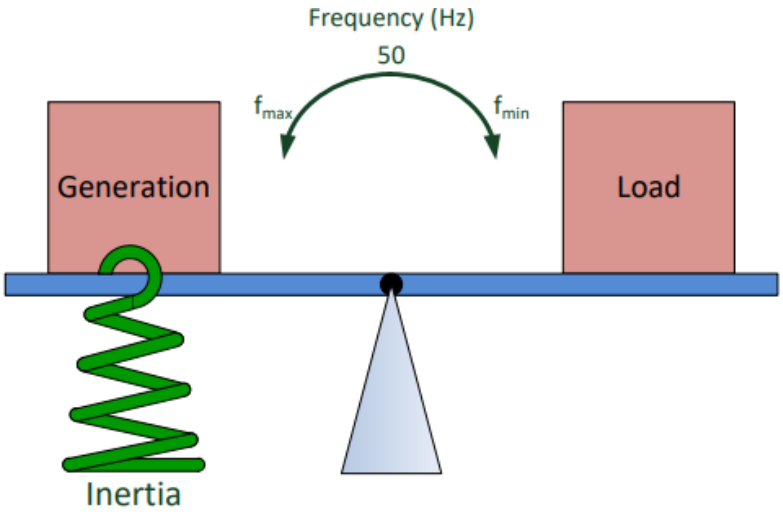

Fig. II.1: The relationship between inertia, generation, and load

II.2.1. Effect of Low Inertia

Low level of inertia in a power system affects system operation and its stability margin. Inertial response, inherent to rotating machines, deteriorates with the rise of inverter-connected RES. Since inertia level defines the rate of frequency deviation in the first seconds after a disturbance, reduced inertia results in faster frequency dynamics. Operation of primary frequency control and protection systems becomes more challenging due to the larger and faster transient frequency deviations [25].

II.3. Concept and Classification of Virtual Inertia Systems

This section discusses the Concept and Classification of Virtual Inertia Systems:

II.3.1. Classification of Virtual Inertia Systems

This section discusses the various topologies that have been proposed in literature. Fig. II. 2 shows a general classification of various topologies that are available in the literature for virtual inertia implementation. Among the listed topologies, the synchronverter, the Ise lab's topology, the virtual synchronous generator (most popular in literature from each classification), and the droop control were selected for a detailed description [26].

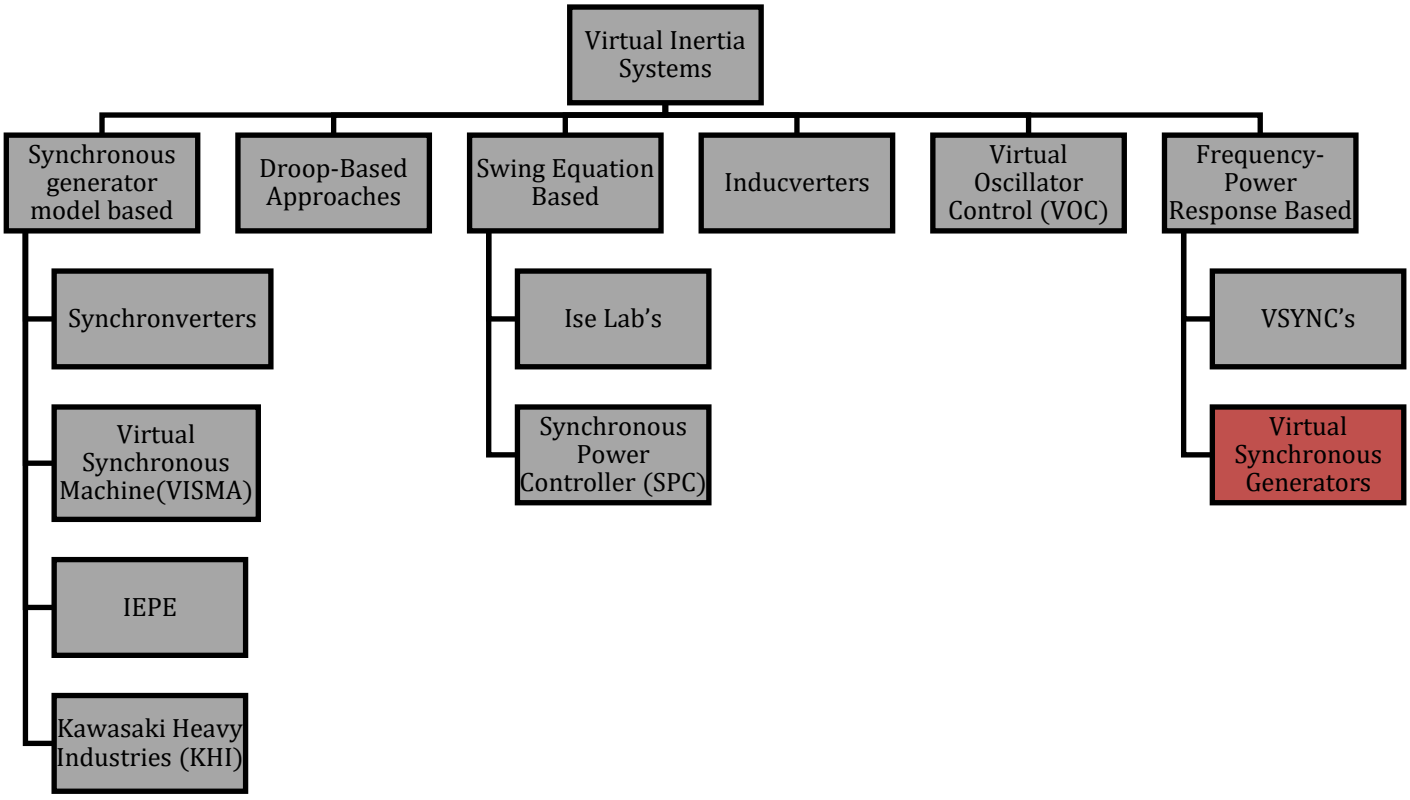

Fig. II.2: Classification of different topologies used for virtual inertia implementation.

II.3.2. Concept of Virtual Inertia Control

The concept of virtual inertia emulation/control is applied to generate the damping and inertia characteristics based on conventional synchronous generation, increasing system inertia/stability and allowing the RESs penetration in frequency control. In this study, it is presumed that the inertia power could be emulated using the combination of the energy storage system ESS, power converter and control technique. Thus, the ESS is essentially an inertial unit, which can adjust the active power of the system, and regulate system frequency through inertia response by changing the control characteristic of the corresponding power converter.

The rate of change of frequency (ROCOF) is known to be affected by system inertia and initial power mismatch .Therefore, ROCOF is computed as follows:

$$\frac{d\omega}{dt} = \frac{\omega^2(T_m - T_e)}{2HS} \qquad \text{(II.4)}$$

The ROCOF can be represented in form of per unit (p.u.) as follows:

$$\frac{d\omega}{dt} = \frac{P_m - P_e}{2HS} \quad \text{(II.5)}$$

In this study, the derivative control technique is the key concept of inertia control, which is able to determine the rate of change of frequency (ROCOF) to modify the extra active power to the set-point value of the system after the disturbance/RES penetration. To obtain the real behavior of the ESS, the low pass filter is added to the system, providing dynamic response. The filter-based low-pass type could also eliminate the noise problem caused by frequency measurements, since the derivative control is very sensitive to the noise. The limiter block is applied to restrict the mini-mum/maximum power capacity of the ESS, representing the practical energy condition of the ESS [27].

Energy Storage System The energy storage system (ESS) has been implemented in various physical realizations. The technology can be directly incorporated into frequency-response services and support the RoCoF during a frequency event. For the last decade, ESSs have become a crucial component in renewable energy integration because they may offer frequency smoothness and balance for future dispatch [28].

The simplified ESS model can be represented as follows:

$$G\ (s) = \frac{1}{1 + sT_{VI\ ,i}} \quad \text{(II.6)}$$

Therefore, the dynamic equation for imitating virtual inertia power is evaluated using:

$$\Delta P_{inertia} = \frac{K_{VI\ ,i}}{1 + sT_{VI\ ,i}} \left[\frac{d(\Delta f_i)}{dt}\right] \quad \text{(II.7)}$$

Where K_{VI} means the virtual inertia constant, T_{VI} means the virtual inertia time constant of the added filter for imitating the dynamic behavior of the ESS, and Δf means the system frequency deviation.

The dynamic model in (Fig. II.3) can virtually emulate the desired inertia power and characteristic to the studied microgrid during the disturbance/RESs penetration, increasing the whole system inertia, frequency performance and stability.

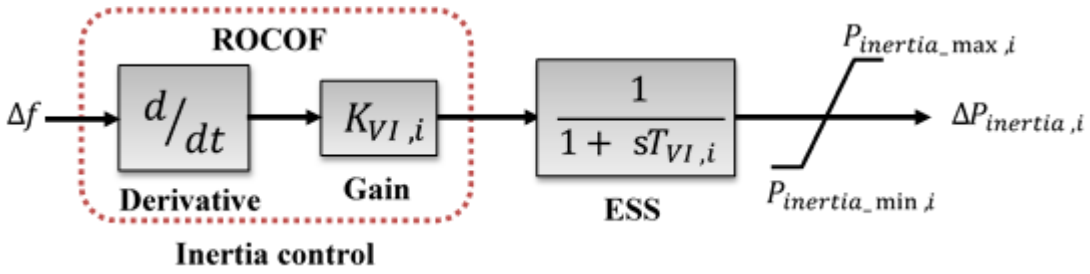

Fig. II.3: Dynamic model of the designed controller for virtual inertia emulation

II.4. PID Regulator

A PID Controller can be described as an extreme form of a phase lead-lag compensator with one pole at its origin and the other at infinity. Similarly, its relatives, the PI and the PD regulators, can also be regarded as extreme forms of phase-lag and phase-lead compensators, respectively [29]. A standard PID controller is also known as the "three-term" controller, whose transfer function is generally written in the "parallel form" given by:

$$G_S = K_P + K_I \frac{1}{s} + K_D s \qquad \text{(II.8)}$$

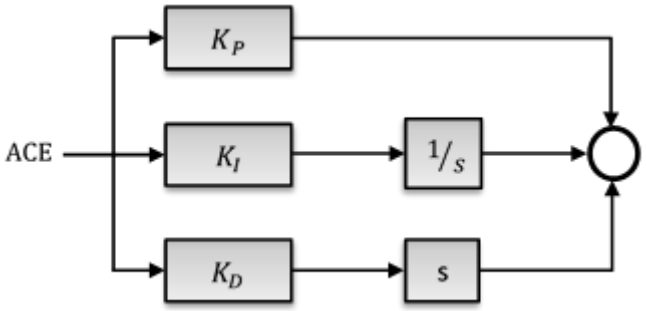

Fig. II.4: PID control scheme "parallel form"

Where K_P is the proportional gain, K_I is the integral gain, K_D is the derivative gain. The "three-term" functionalities are highlighted by the following [29]:

- The proportional term K_P: providing an overall control behavior equals the error signal through the all-pass gain factor.
- The integral term K_I: reducing steady-state errors through low-frequency compensation by an integrator.
- The derivative term K_D: improving transient response through high-frequency compensation by a differentiator.

II.5. The Global System with the Proposed Controllers

In this section, we are going to represent AGC two-area interconnected thermal power system with the presence of RESs. Each area composed by speed governing system, turbine, generator, GDB and GRC. Controlled by VIC and PID in each area.

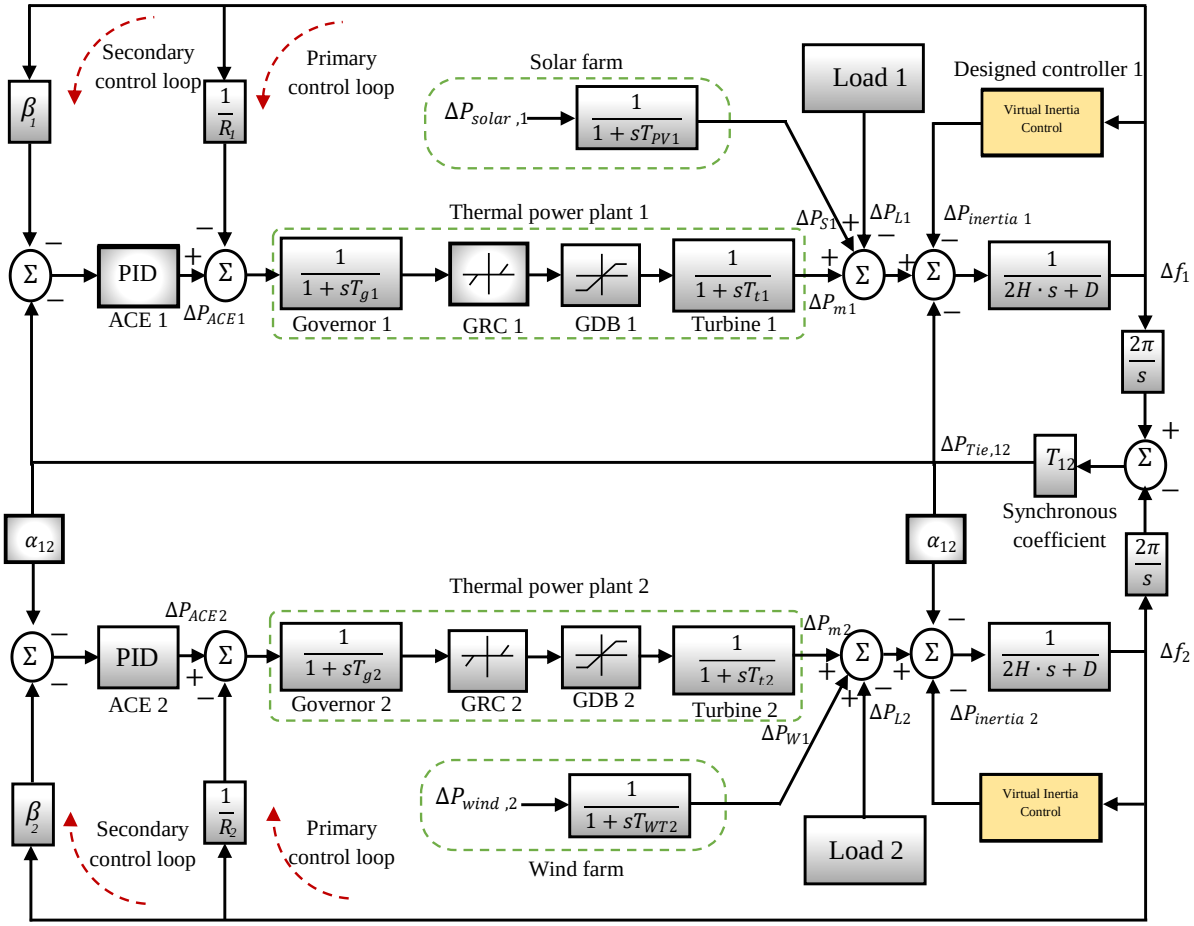

Fig. II. 5: Dynamic model of AGC two-area power system with the present of virtual inertia control and PID controller.

II.6. Optimization of regulator parameters

In the design and analysis of control systems, some configuration requirements are needed to reduce the system's steady state error. The optimum value of controller parameters is obtained by minimizing a specified objective function. The device synthesis method uses several parameters. (Fig. II.6) flowchart describes the different output parameters used for controller synthesis [30].

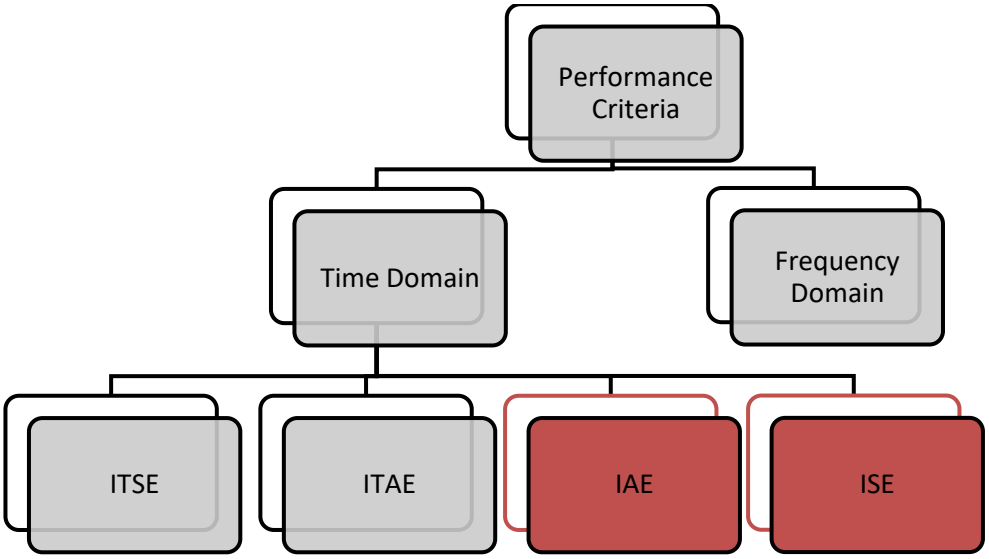

Fig II.6: Different existing performance criteria

- **Integral of square error**

We use the Integral of Square Error (ISE) performance index for the performance evolution of PID controller. The following equation shows its function:

$$J = ISE = \int_0^{\infty} e^2(t)dt \qquad \text{(II.9)}$$

For n areas power system, the error e(t) is represented by:

$$\mathrm{e(t)} = \sum_{i=1}^{n} ACE_i \qquad \text{(II.10)}$$

Where (t) needs to be minimized.

- **Integral of the absolute error**

The Integral Absolute Error (IAE) is the suitable performance index examined here and it is presented by:

$$J = IAE = \int_0^{\infty} |e(t)|\, dt \qquad \text{(II.11)}$$

II.7. Optimization

II.7.1. What is optimization?

Maximizing or minimizing some of the functions in relation to a set, often representing a range of choices available in a given situation. The function allows a comparison of the different choices for determining which may be "best" [31].

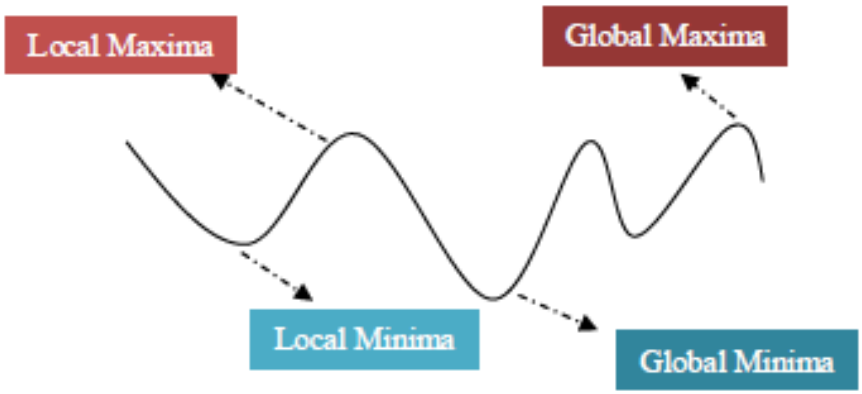

Fig. II.7: Local and Global Optimal Solution

Common applications: minimum cost, maximum profit, best approximation, optimum design, optimal management or control, variation principles.

II.7.2. Classification

Optimization technics can be classified in many ways, following figure presents the classification of it [32].

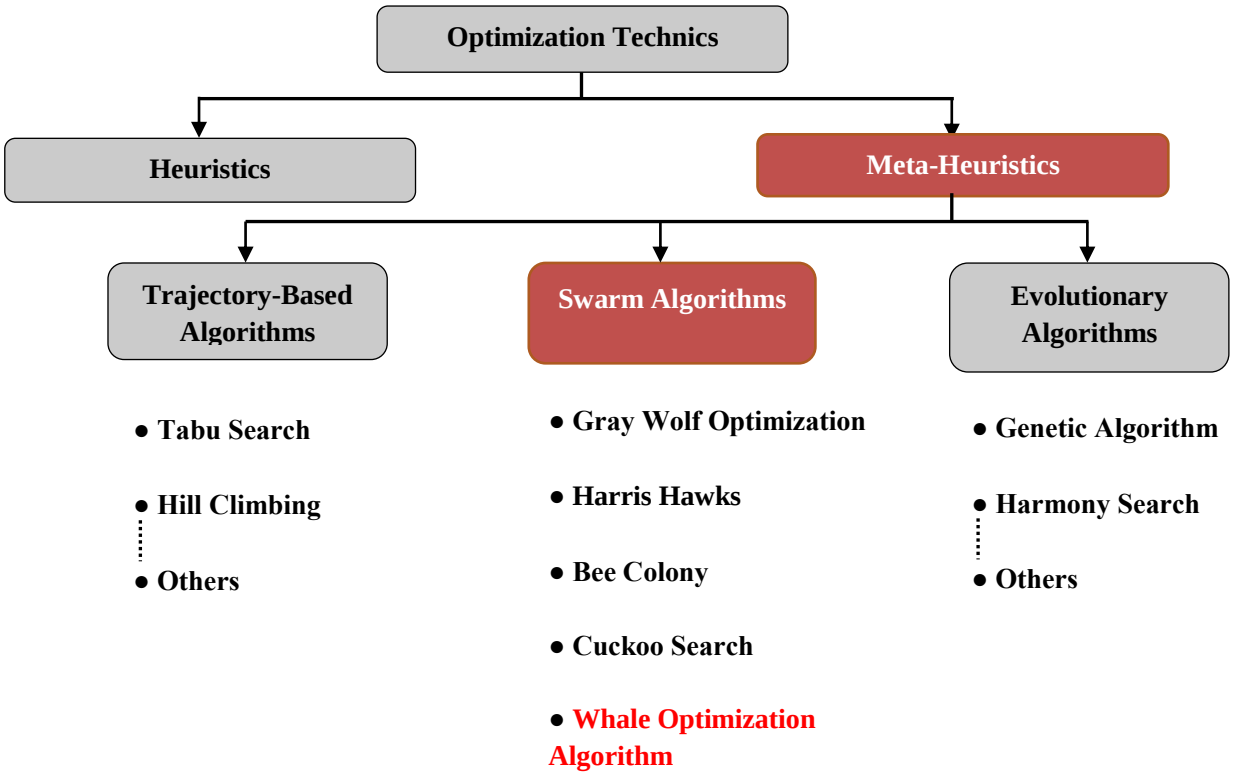

Fig II.8**:** Classification of optimization technics

II.7.2.1. Meta-heuristics

The new paradigms were called metaheuristics and were first introduced at mid-80s as a family of searching algorithms able to approach and solve complex optimization problems, using a set of several general heuristics. The term metaheuristic is define a high-level heuristic used to guide other heuristics for a better evolution in the search space. Although traditional stochastic search methods are mainly guided by chance (solutions change randomly from one-step to another), they can be used in combination with metaheuristic algorithms to guide the search process and to accelerate the convergence.

Most metaheuristics algorithms are only approximation algorithms, because they cannot always find the global optimal solution. However, the most attractive feature of a metaheuristic is that its application requires no special knowledge on the optimization problem to be solved, hence it can be used to define the concept of general problem solving model for optimization problems or other related problems [33].

Any meta-heuristic algorithm has two major components which are diversification and intensification, or also known as exploration and exploitation. We can say that diversification means to generate diverse solutions so as to explore the search space on a global scale, while intensification means to focus the search in a local region knowing that a current good solution is found in this region. Thus, during the selection of the best solution, a good balance between diversification and intensification should be found to improve the rate of algorithm convergence, and it generally ensures that a global optimality is achievable [34].

In our case of study, we are going to use Whale Optimization Algorithm (WOA) method which is classified with the meta-heuristic swarm algorithms.

II.8. Whale Optimization Algorithm

Whale optimization algorithm was proposed by Jalili and Lewis for optimizing numerical problems (Mirjalili & Lewi, 2016). The algorithm simulates the intelligence hunting behavior of humpback whales. This foraging behavior is called bubble-net feeding method that is only be observed in humpback whales. The whales create the typical bubbles along a circle path while encircling prey during hunting. Simply, bubble-net hunting behavior could describe such that humpback whales dive down approximation 12 m and then create the bubble in a spiral shape around the prey and then swim upward the surface following the bubbles [35].

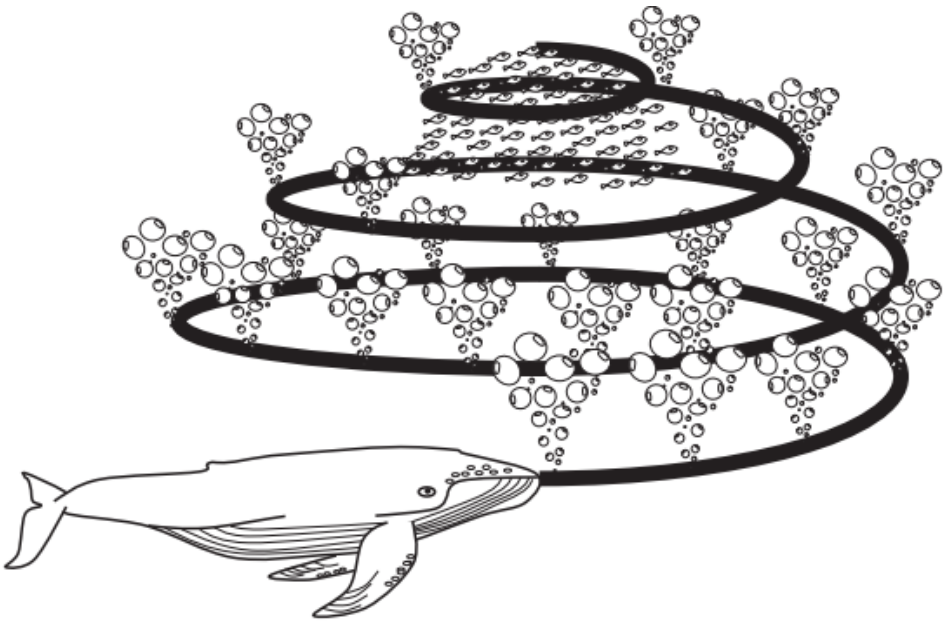

Fig. II.9: Bubble-net feeding behavior of humpback whales.

II.8.1. Mathematical model and optimization algorithm

In this section the mathematical model of encircling prey, spiral bubble-net feeding maneuver, and search for prey is first provided. The WOA algorithm is then proposed [36].

a. Encircling prey

In the WOA, the prey position is considered as a candidate solution. The encirclement of the humpback whales to the prey can be formulated by the following formulas:

$$\vec{D} = \left|\vec{C} \cdot \overrightarrow{X^*}(t) - \vec{X}(t)\right| \quad \text{(II.12)}$$

$$\vec{X}(t+1) = \overrightarrow{X^*}(t) - \vec{A} \cdot \vec{D} \quad \text{(II.13)}$$

Where t indicates the current iteration, $\vec{A}$ and $\overrightarrow{C}$ are coefficient vectors, $\vec{X}*$ is the prey position vector, $\vec{X}$ is the whale's position vector.

The vectors $\vec{A}$ and $\overrightarrow{C}$ are calculated as follows:

$$\vec{A} = 2\vec{a} \cdot \vec{r} - \vec{a} \quad \text{(II.14)}$$

$$\vec{C} = 2 \cdot \vec{r} \quad \text{(II.15)}$$

Where $\vec{a}$ is linearly decreased from 2 to 0 over the course of iterations (in both exploration and exploitation phases) and $\vec{r}$ is a random vector, which lies in the range of 0 and 1.

b. Bubble-net attacking method (exploitation phase)

The Bubble-net strategy is hybrid of combined two approaches that can be mathematically model as follows:

- **Shrinking encircling mechanism**

In this approach, the whales swim around the prey in shrinking circles. This can be achieved by decreasing ***a*** from 2 to 0 with iterations and $|A| < 1$.

- **Spiral updating position**

In this approach, a spiral equation is created between the position of whale and prey to simulate the helix-shaped movement of humpback whales as follows:

$$\vec{D}' = \left|\overrightarrow{X^*}(t) - \vec{X}(t)\right| \quad \text{(II.16)}$$

$$\vec{X}(t+1) = \vec{D}' \cdot e^{bl} \cdot \cos(2\pi l) + \overrightarrow{X^*}(t) \quad \text{(II.17)}$$

Where $\vec{D}'$ is the distance between the whale and prey, *b* is a constant that determines the spiral logarithmic shape, *l* is a random number lies in the range of −1 and 1 [35]

The whales exhibit the two approaches simultaneously during the attacking process. Therefore, it is assumed that they do shrinking encircling mechanism by a probability of 50% and the spiral model by the same probability to update their positions [36], which can be modelled as follows:

$$\vec{X}(t+1) = \begin{cases} \overrightarrow{X^*}(t) - \vec{A} \cdot \vec{D}, & if\ p < 0.5 \\ \vec{D}' \cdot e^{bl} \cdot \cos(2\pi l) + \overrightarrow{X^*}(t), & if\ p \geq 0.5 \end{cases} \quad \text{(II.18)}$$

Where *p* is a random number in [0,1].

- **Search for prey (exploration phase)**

In this process, the humpback whales search for the prey and this presents the exploration or global search of the WOA. It is found that $|A| > 1$ can express the search process [36]. The whales or the agent's position can be updated as follows:

$$\vec{D} = \left|\vec{C} \cdot \overrightarrow{X_{rand}} - \vec{X}\right| \quad \text{(II.19)}$$

$$\vec{X}(t+1) = \overrightarrow{X_{rand}} - \vec{A} \cdot \vec{D} \quad \text{(II.20)}$$

Where $\overrightarrow{X_{rand}}$:is a random position vector (a random whale) chosen from the current population.

II.8.2. WOA Algorithm

The algorithm of this WOA is reported as follows [36]:

WOA's Algorithm

Initialize the whales population Xi (i = 1, 2, ..., n)

Calculate the fitness of each search agent

X=the best search agent*

while *(t < maximum number of iterations)*

for *each search agent*

Update a, A, C, l, and p

if1 *(p<0.5)*

if2 *(|A|< 1)*

*Update the position of the current search agent by the Eq. (*II.12*)*

else if2 *(|A| ≥ 1)*

Select a random search agent (X_{rand})

*Update the position of the current search agent by the Eq. (*II.20*)*

end if2

else if1 *(p ≥ 0.5)*

*Update the position of the current search by the Eq. (*II.17*)*

end if1

end for

Check if any search agent goes beyond the search space and amend it

Calculate the fitness of each search agent

Update X if there is a better solution*

t=t+1

end while

*return X**

II.9. Conclusion

This chapter provides the VIC used for the design purpose of controllers in the inertia problem. At the start, some details about inertia with their effect in power systems and the concept and classifying of virtual inertia systems. After that, we have provided different existing performances criteria which can be used in optimization of regulator parameters. Finally and after defining the optimization and classifying the meta-heuristics, a method called Whale optimization algorithm (WOA) was chosen for our case study and explained in details.

CHAPTER III:

Simulation and Results

III.1. Introduction

In this chapter, we will provide the effectiveness of using VIC in the AGC problem. The investigations are carried out in two-area reheat system with RESs (solar, wind) and taking in consideration GDB and GRC for more realistic case of study. Firstly, we will discuss the effect of inertia on the global response of the frequency without VIC. Then, we will observe the performance of VIC in the system providing all the dynamic response of the microgrid. After that, we will compare the change of inertia in the system while VIC is present to the system without VIC. Lastly, a severe test is applied to see how the VIC can improve the system and make it more robust. The optimum PID settings of AGC without and with VIC are determined through a new optimization algorithm called WOA by evaluating two dynamic criteria such as ISE and IAE.

III.2. Investigated power system

The system of our study case involves two-area interconnected thermal power system with the presence of RESs. Each area composed by speed governing system, turbine, generator, GDB and GRC, Solar power generation in area-1and Wind power generation in area-2. We consider 1.5 MW load variation in area 1 ($\Delta PL1$= 0.1 *p.u.*) in all study. The parameters of the nominal system and VIC are taken from the appendix.

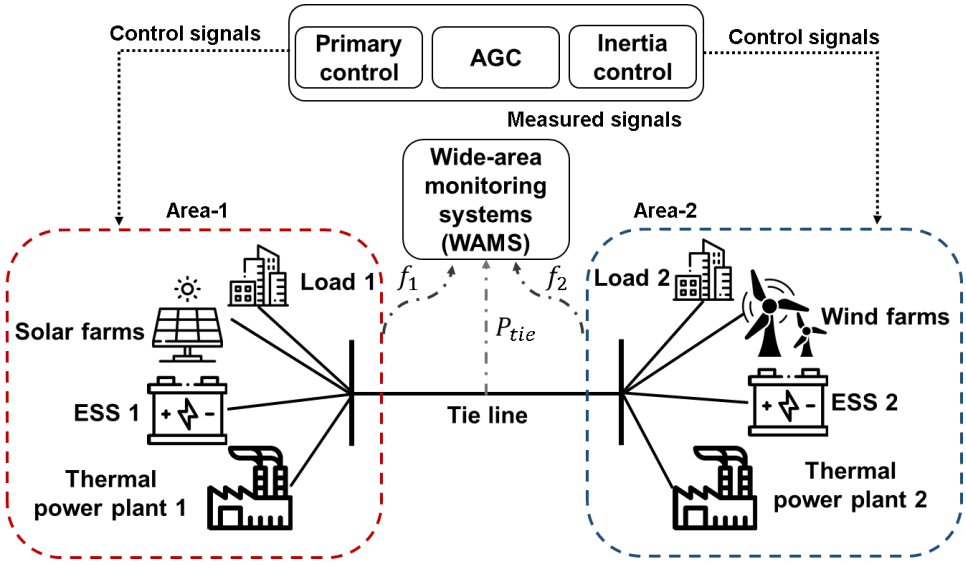

Fig. III.1: Two areas investigated study system

III.3 Discussion

In this study, simulations have been performed by MATLAB/SIMULINK on the two areas thermal system as seen in Fig. III.1. After several tests, the optimum controller parameters of PID and VIC were obtained by executing the WOA for the system without and with VIC evaluating both ISE and IAE, all according 0.1 *p.u.* load variation in area 1.

III.3.1. The Effect of Inertia H Without VIC

In this section, we want to test the effect of inertia on the system without the presence of VIC. The test is considered by changing the value of H in the system by a step of 25% from its nominal value (starting from -50% -25% 0% +25% +50%).

This comparison is made under the same values of PID controller parameters as shown in table III. 1 for ISE criterion, table III. 2 for IAE criterion. The frequency responses in area 1 are shown in Fig. III. 2 (a, b) for ISE and IAE criterion respectively.

Table III. 1: optimal values of PID parameters for ISE criterion

Controller Gain	K_P	K_I	K_D
Area 1	9.8809	9.6061	3.3542
Area 2	9.8809	9.8809	9.8809

Table III. 2: optimal values of PID parameters for IAE criterion

Controller Gain	K_P	K_I	K_D
Area 1	10.00	10.00	2.7131
Area 2	10.00	10.00	7.5653

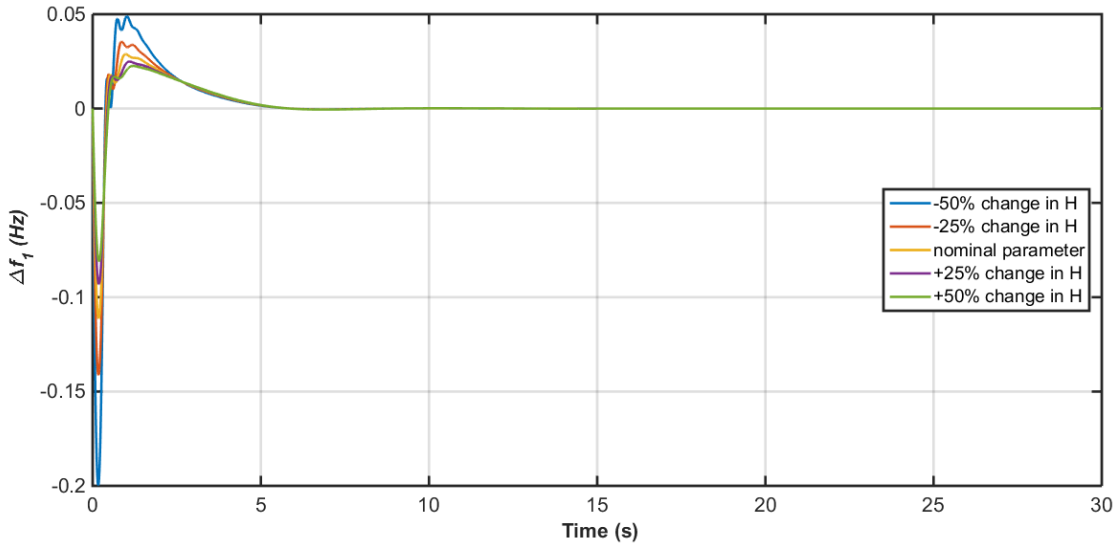

(a)

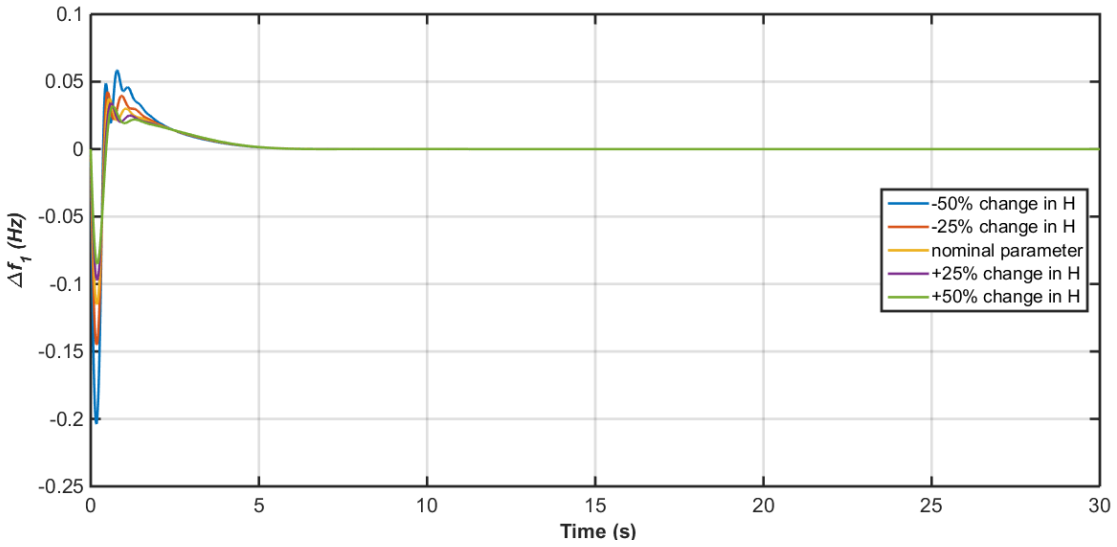

(b)

Fig. III.2: Frequency response in area 1 (a): With ISE Criterion (b): with IAE criterion

It is noticeable that the inertia H has a significant effect on the frequency response. We can see that when H is decreased the peak overshoot (PO) and undershoot (PU) of frequency deviation is greater than its nominal value. In addition, it is obvious that inertia makes the system more stable and robust for the reason that the PO and PU is decreased when H it is increased.

III.3.2. Abrupt Load Change

For this part, a comparison is done for the proposed interconnected power system without VIC and With VIC with the nominal H. The parameters of PID and VIC are optimized all together to

get a better result. The optimal setting of PID and VIC are provided in table III.3 for the system with VIC evaluating ISE criterion and table III.4 for IAE criterion.

Table III.3: Optimal settings of PID and VIC for ISE criterion.

Controller Gain	K_P	K_I	K_D	K_{VIC}
Area 1	10.0000	10.0000	3.0559	10.0000
Area 2	10.0000	10.0000	4.1483	10.0000

Table III.4: Optimal settings of PID and VIC for IAE criterion.

Controller Gain	K_P	K_I	K_D	K_{VIC}
Area 1	10.0000	10.0000	1.3710	10.0000
Area 2	10.0000	10.0000	7.9118	5.3932

The values of ISE and IAE criterion of the frequency response in both cases of the system without and with VIC are shown in Fig. III.3 (a, b) respectively.

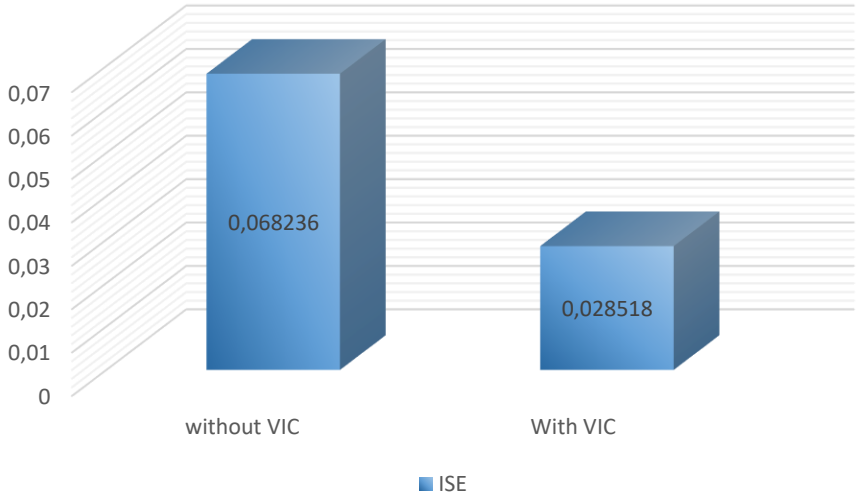

(a)

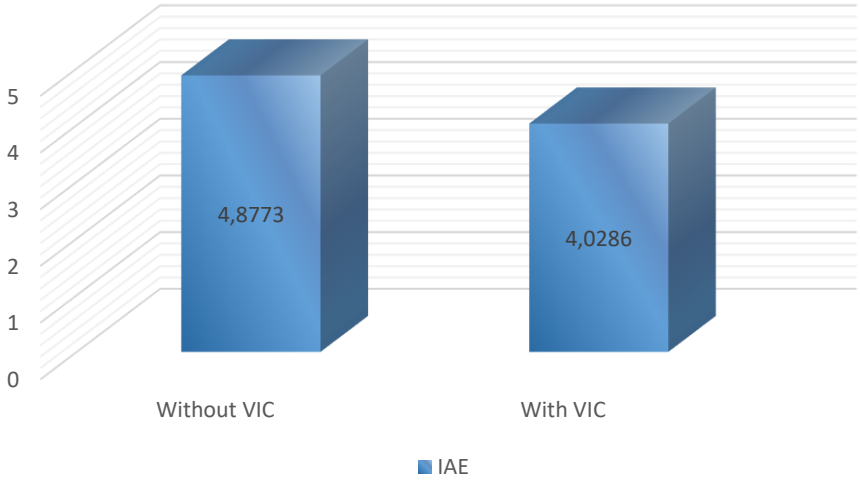

(b)

Fig. III.3: Comparison of the system with and without VIC. (a) ISE criterion (b) IAE criterion

From Fig. III.3 we can clearly notice the difference caused by the presence of VIC in the system with high RESs penetration. It is obvious that the value of ISE criterion has been reduced by 58,2% when VIC is implemented in the interconnected power system. After that, we can see that the IAE criterion value of the system without VIC is increased by 17,4% compared to with VIC. Fig. III. (4-7) (a and b) represent all areas dynamic responses of frequency deviation (Δf_i), Area Control Error (ACE_i), mechanical power deviation (ΔPm_i) and tie line power deviation (ΔP_{tie12}), obtained by ISE criterion respectively.

Fig. III.8 (a, b, c and d) represent all dynamic responses of frequency deviation (Δf_1), Area Control Error (ACE_1), mechanical power deviation (ΔPm_1) and tie line power deviation (ΔP_{tie12}), obtained by IAE criterion in area 1 respectively.

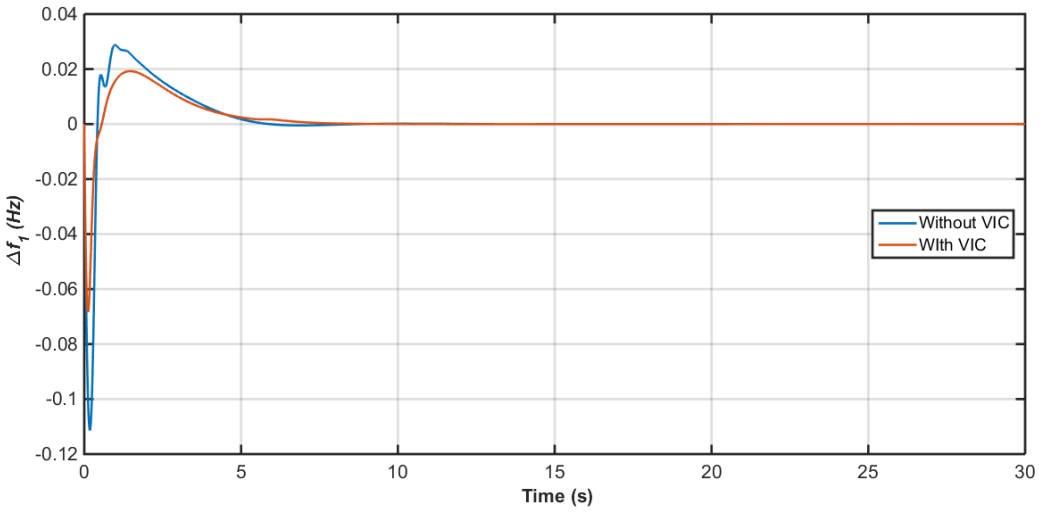

(a)

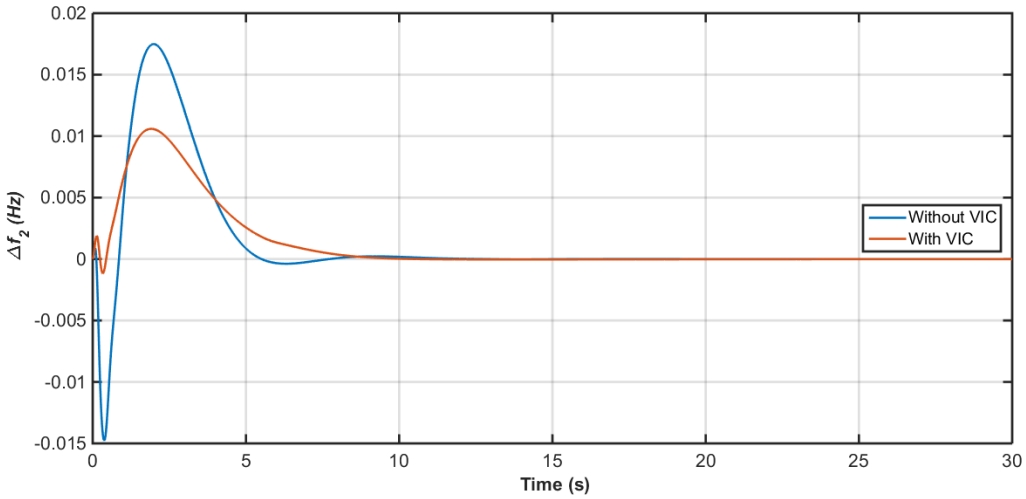

(b)

Fig. III.4: Frequency deviation (Δf_i) without/with VIC, (a): area-1 (b): area-2 using ISE criterion

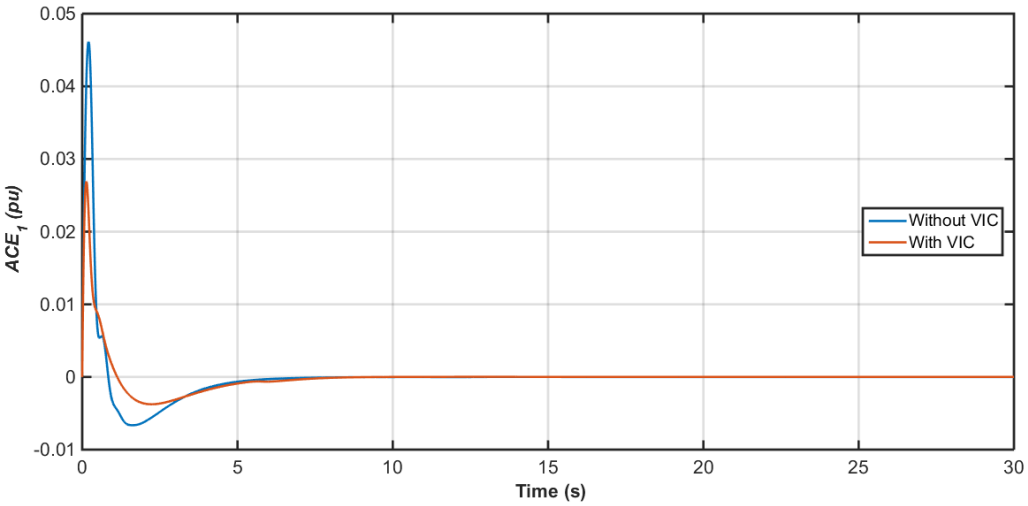

(a)

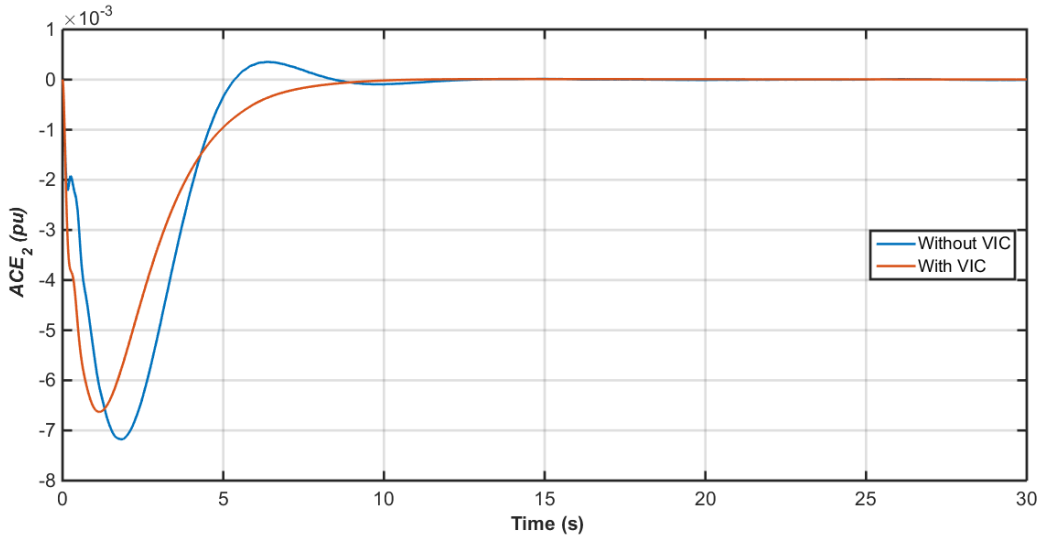

(b)

Fig. III.5: Area control error (ACE_i) without/with VIC, (a): area-1 (b): area-2 using ISE criterion

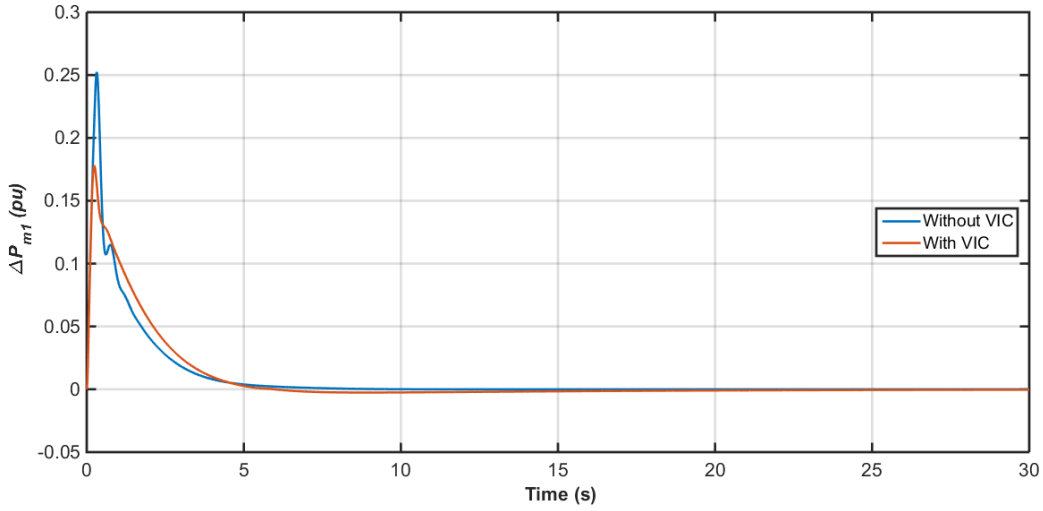

(a)

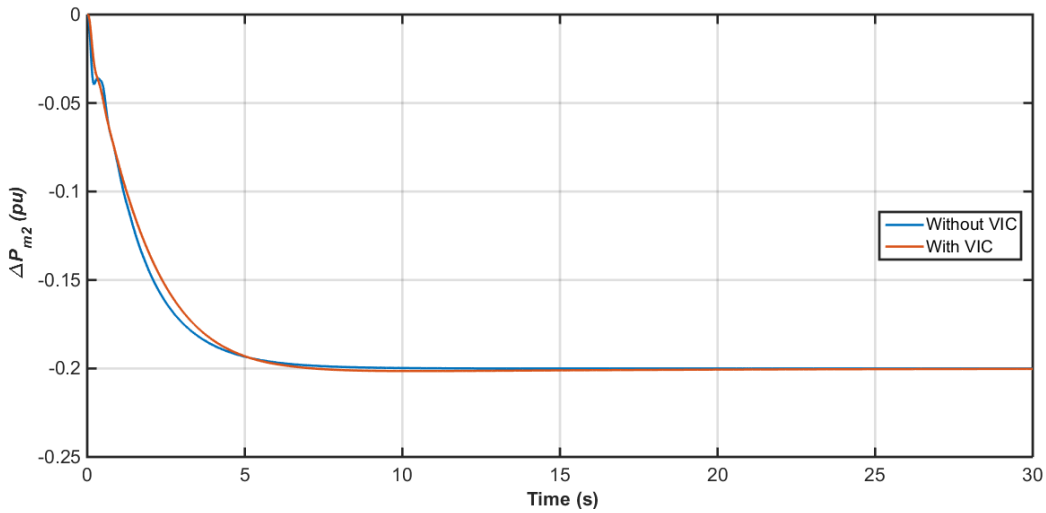

(b)

Fig. III.6: Mechanical power deviation (ΔPm_i) without/with VIC, (a): area-1 (b): area-2 using ISE criterion

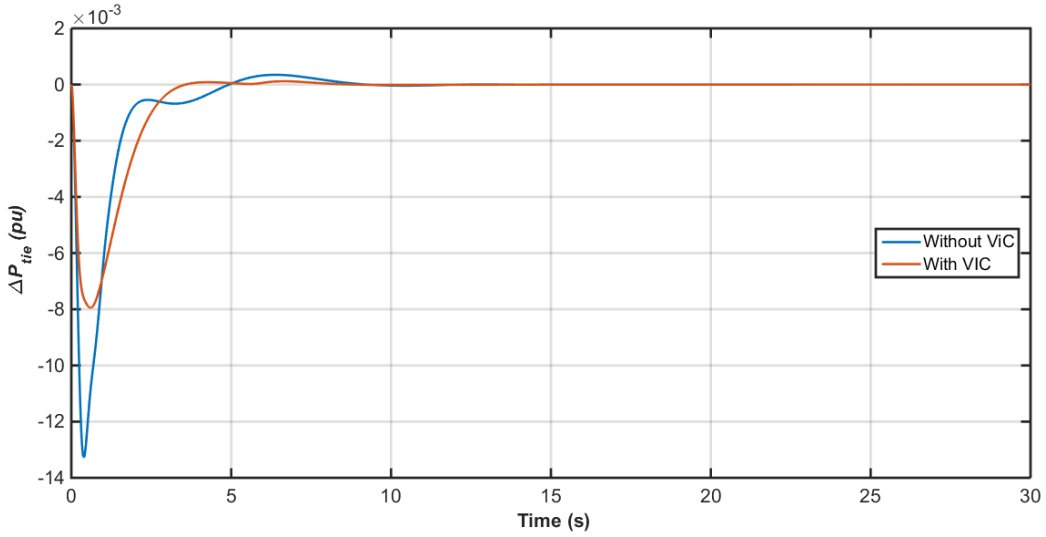

Fig. III.7: Tie line power deviation (ΔP_{tie12}) without/with VIC

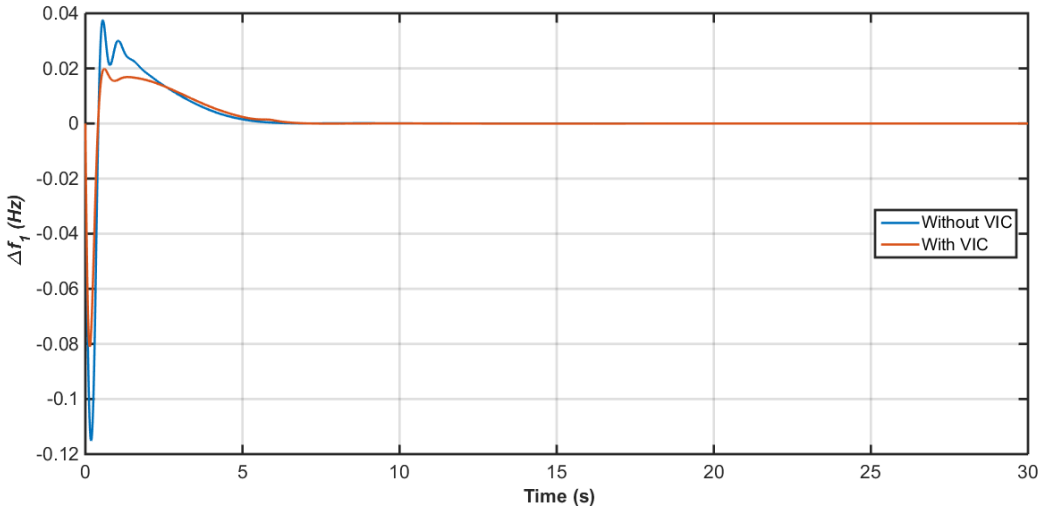
0.04
0.02
0
-0.02
-0.04
-0.06
-0.08
-0.1
-0.12
Δf_1 (Hz)
0
5
10
15
20
25
30
Time (s)
Without VIC
With VIC

(a)

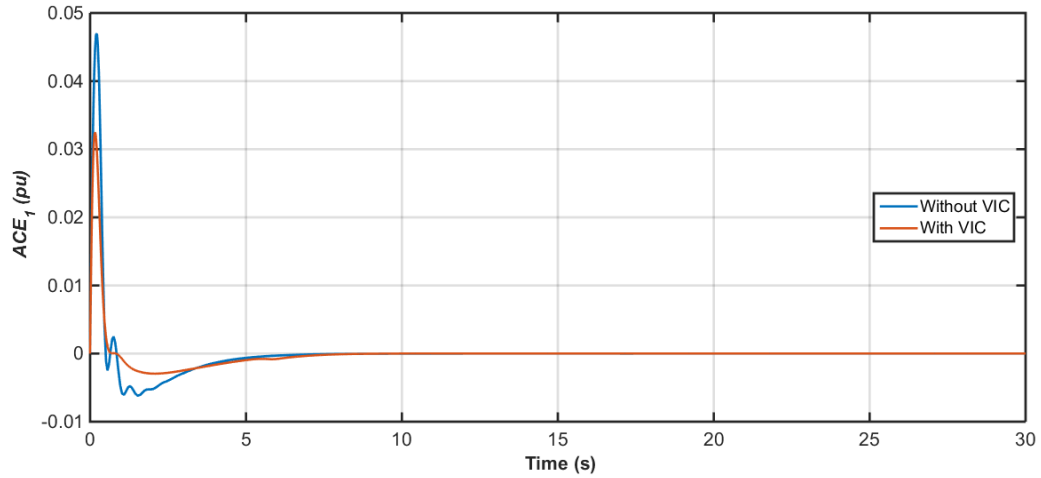
0.05
0.04
0.03
0.02
0.01
0
-0.01
ACE_1 (pu)
0
5
10
15
20
25
30
Time (s)
Without VIC
With VIC

(b)

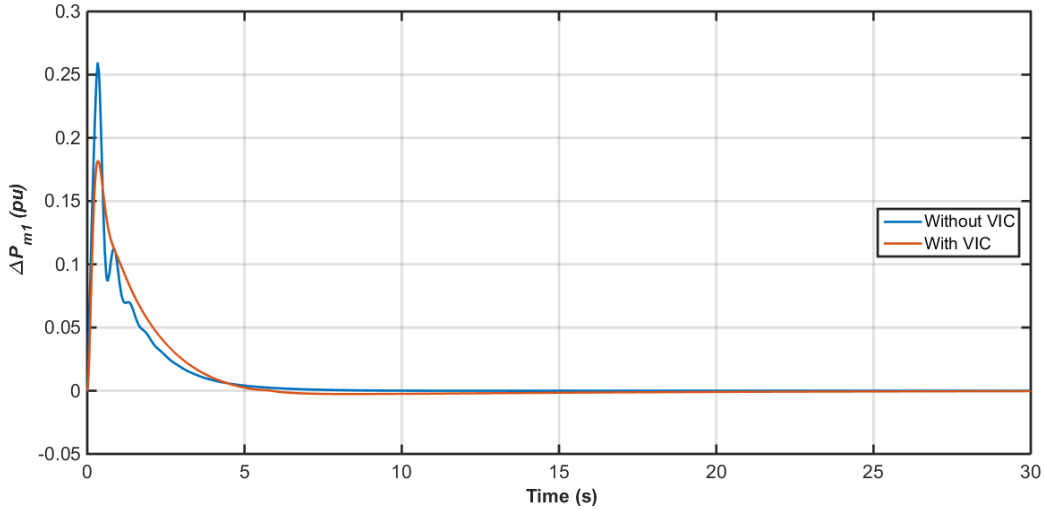
0.3
0.25
0.2
0.15
0.1
0.05
0
-0.05
ΔP_{m1} (pu)
0
5
10
15
20
25
30
Time (s)
Without VIC
With VIC

(c)

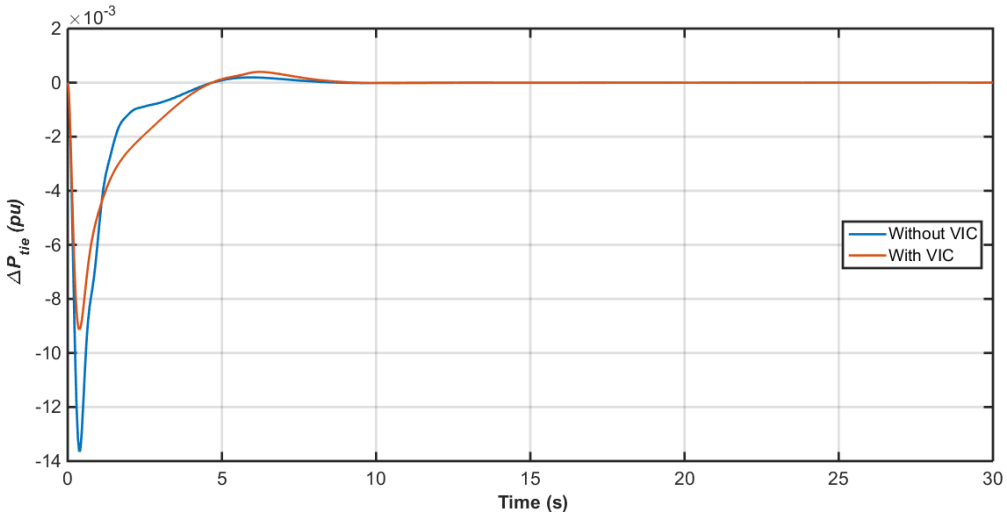

(d)

Fig. III.8: Dynamic responses (a): Frequency deviation (Δf_1), (b): Area Control Error (ACE_1), (c): Mechanical power deviation (ΔPm_1) and (d): Tie line power deviation (ΔP_{tie12}), obtained by IAE criterion in area 1

These figures can show the change caused by integrating VIC into a system with high RESs penetration levels. It is easily observed that VIC has enhanced all the dynamic responses of the interconnected power. The frequency response was fast which makes the interconnected power system more stable in terms of settling time (ST), peak overshoot (PO) and peak undershoot (PU). Even the tie line power deviation was less unsteady in the presence of VIC. According to these results we can conclude that VIC can directly contribute in the stability of the system and decrease the sensitivity of the microgrid to several unpredicted contingencies.

The results were obtained using HHO to find the optimal control settings based on ISE and IAE criterion. If we compare the results between ISE and IAE, we can notice that using ISE criterion might lead to better parameter gains, for the reason that the dynamic responses of the system using the parameters obtained from evaluating ISE criterion proved to be slightly better.

III.3.3. The Effect of Inertia H With VIC

In section III.3.1, we tested inertia of the system without VIC. Now, the same test is carried out in this part but with the presence of inertia using the same controller parameters in table III.3 and table III.4. Fig. III.9 (a, b) shows the frequency deviation of the system with VIC using ISE and IAE criterion respectively with changing the value of H in the system by a step of 25% from its nominal value (starting from -50% -25% 0% +25% +50%).

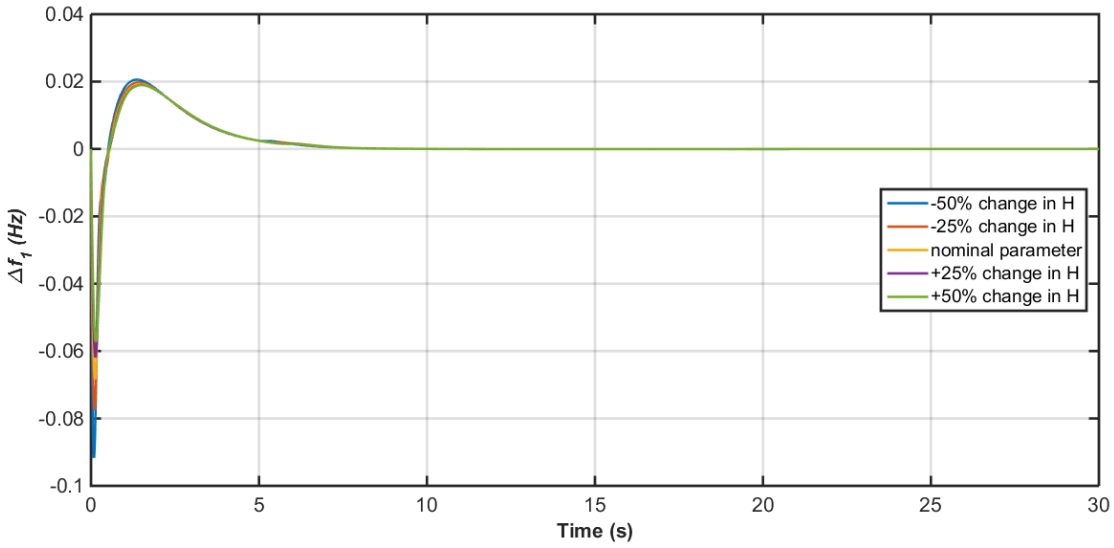

(a)

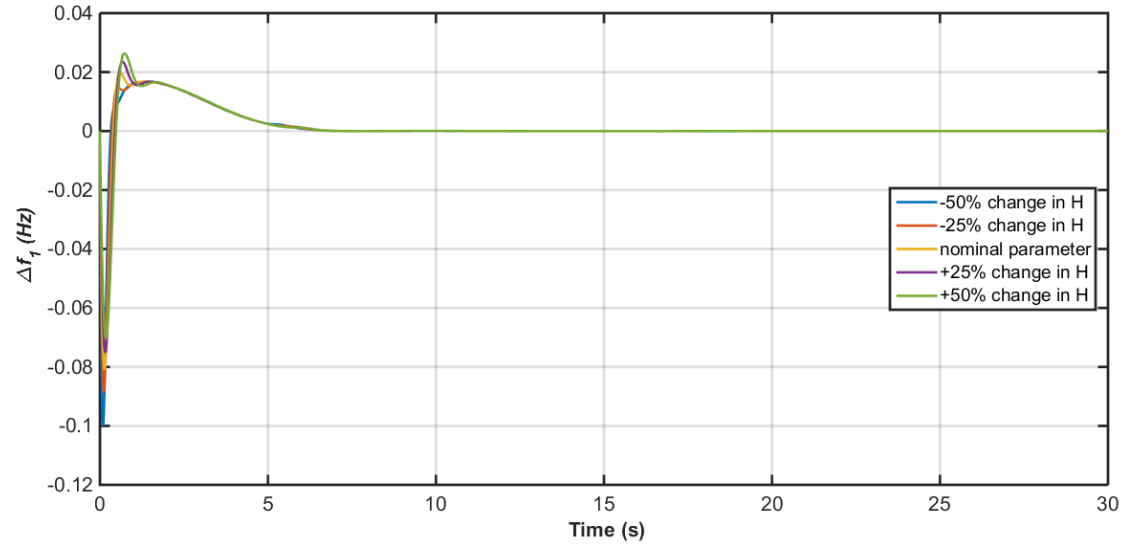

(b)

Fig. III.9: Frequency response in area 1 (a): With ISE Criterion (b): with IAE criterion

From Fig. III.9 we can see that H has an effect on the response of the system even in the presence of VIC. But we can notice the difference caused by VIC. The deviation of frequency is less with VIC even though the steps of change in the inertia are same of section III.3.1. Hence, comparing the results obtain in Fig.III.9 to the ones of Fig. III.2, it is noticeable that the system is more sensitive to the change of H when VIC is absent. Then, the VIC can make the system more robust even in a low inertia environment.

III.3.4. Random RESs Generation and Load Disturbances

To perform a more severe simulation and test the robustness of proposed VIC technics, the interconnected power system is evaluated under the conditions of random and different load and RESs disturbances.

Fig. III.10 presents the random RESs generation and load power disturbances patterns and the dynamic response of the frequency deviation is provided in Fig.III.11.

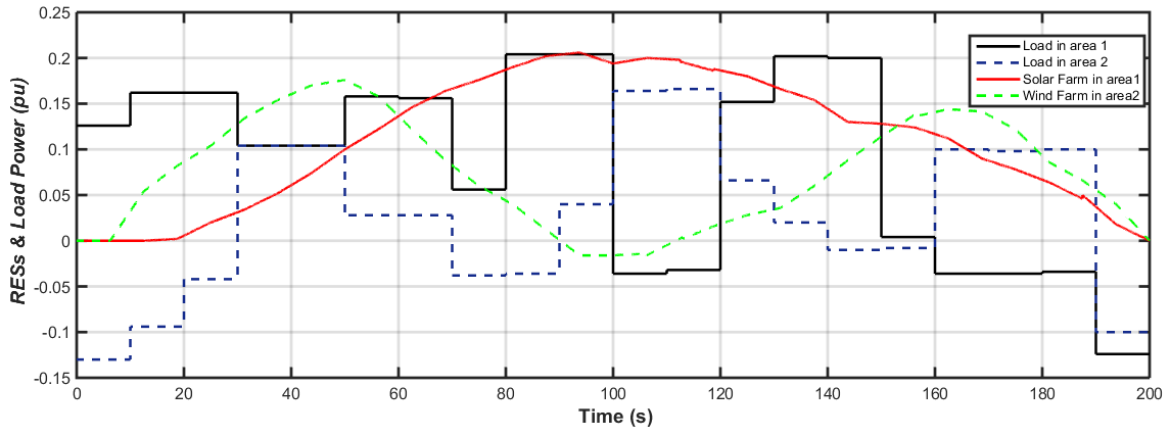

Fig. III.10: Random RESs generation and load power disturbances patterns

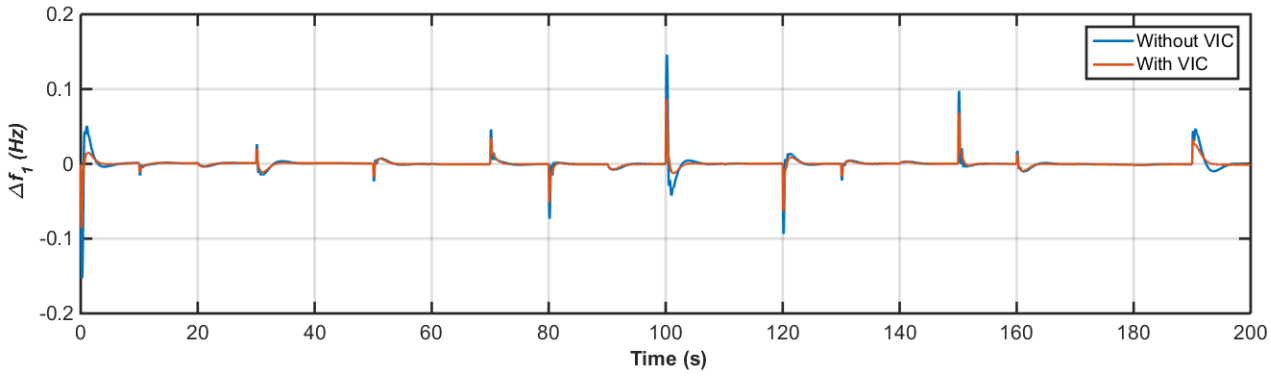

Fig.III.11: The dynamic response of the frequency deviation in area 1

This test is a proof that the VIC is a reliable solution for the low inertia problem, because it could maintain the best response even under severe RESs penetrations and random load disturbances. The frequency response is way better when integrating VIC into the system from the view of PO, PU and ST.

III. 4 Conclusion

We went through in this chapter by two parts. First part is the proposed study system provided with its parameters. Then the second part is the discussion part where we started with testing the system by changing inertia to understand its effect. After that, a comparison between the suggested system with and without VIC was carried out under an abrupt load change. Hence, VIC proved to be a reliable solution to the low inertia problem with its high performance. In addition, the effect of low inertia is reduced in the presence of VIC. Finally, to confirm the robustness and the sensitivity of the system we applied severe random load and RESs changes over time.

GENERAL CONCLUSION

General Conclusion

In this work, a novel application to virtual inertia control-based derivative control techniques is proposed to improve frequency performance and stability of interconnected systems with high RESs penetration. For that reason, we used classical controllers such as PID in the secondary control loop of the AGC problem with determining the optimal controller settings via a novel optimization algorithm known as Whale Optimization Algorithms WOA. Furthermore, we integrated VIC controllers in each area for even a better performance in our proposed system.

We have passed through the following stages to attain our main objective:

First of all, we have explained all needed elements for our memoir such as single and multi-area AGC problem with its well treated control loops. Then, we have seen and explained the RESs models and there effect in our study system.

Secondly, since we wanted to implement VIC controllers in our suggested system, we had to introduce VIC controllers with its models and structures. After that, we defined the used PID for designing the secondary control loop. In addition, to obtain the optimal regulator parameter, we discussed the Whale Optimization Algorithms WOA with details.

At last, the proposed system contains two-area interconnected thermal power system with the presence of two RESs (solar , wind) and VIC in each area. We had two cases of study to put into comparison:

- System without VIC with the changing of the value H to see its effect.
- Abrupt Load Change on the system without/with VIC.
- Integrating VIC in the system with the changing of the value H to compare the results with the first case.
- Random RESs generation and load disturbances to confirm the robustness of the proposed control technic.

This memoir has discussed some important points of control strategies in the LFC problem. For further research, the next suggestions are recommended:

- Implementing control service to extract frequency control support from HVDC interconnections

General Conclusion

- Use of the energy storage devices (ESDs), such as redox flow batteries (RFBs) in the LFC dynamics;
- Implementing supplementary control for frequency control in demand- side during frequency events

References

[1] Kerdphol, T., Watanabe, M., Mitani, Y., & Phunpeng, V. (2019). Applying virtual inertia control topology to SMES system for frequency stability improvement of low-inertia microgrids driven by high renewables. *Energies*, *12*(20), 3902.

[2] G. Sharma, K. Loji, M. Kabeya, "Application of Diverse FACTS in AGC of Multi-Area Interconnected Energy Systems" Department of Electrical Power Engineering, Durban University of Technology, South Africa, June 2019.

[3] Ejegi, E. E., Rossiter, J. A., & Trodden, P. (2014, July). A survey of techniques and opportunities in power system automatic generation control. In *2014 UKACC International Conference on Control (CONTROL)* (pp. 537-542). IEEE.

[4] Said, S. M., Aly, M., Hartmann, B., & Mohamed, E. A. (2021). Coordinated fuzzy logic-based virtual inertia controller and frequency relay scheme for reliable operation of low-inertia power system. *IET Renewable Power Generation*, *15*(6), 1286-1300.

[5] Tebib, A., & Boudour, M. (2021). Stability improvement of interconnected AC/DC multiarea AGC power systems using optimized virtual synchronous power strategy based on eigenvalues sensitivity and adaptive mixed GWO. *International Transactions on Electrical Energy Systems*, *31*(4), e12725.

[6] Singh, O., Tiwari, P., & Singh, A. (2013). A survey of recent automatic generation control strategies in power systems. *International Journal of Emerging Trends in Electrical and Electronics*, *7*(2), 1-14.

[7] Li, M., Huang, W., Tai, N., & Duan, D. (2021). Virtual Inertia Control of the Virtual Synchronous Generator: A Review. *arXiv preprint arXiv:2109.07590*.

[8] H. Kwatny, K. Kalnitsky, and A. Bhatt, "An Optimal Tracking Approach to Load Frequency Control," IEEE Trans. Power App. Syst., Vol. PAS-94, no. 5, pp. 1635–1643, Sep./Oct. 1975.

[9] R. Dey, S. Ghosh, G. Ray, A. Rakshit, "H∞ Load Frequency Control of Interconnected Power Systems with Communication Delays," Electrical Power and Energy Systems 2012.

[10] T. Bechert, N. Chen, “Area Automatic Generation Control by Multi-Pass Dynamic Programming,” IEEE Trans. Power App. Syst., vol. PAS-96, no. 5, pp. 1460–1468, Sep./Oct. 1977.

[11] D. Das, J. Nanda, M. Kothari, and D. P. Kothari, “Automatic Generation Control of Hydrothermal System with New Area Control Error Considering Generation Rate Constraint,” Elect. Mach. Power Syst., vol. 18, no. 6, pp. 461–471, Nov. /Dec. 1990.

[12] Bevrani, H., Daneshfar, F., & Hiyama, T. (2012). *A new intelligent agent-based AGC design with real-time application*. IEEE Transactions on Systems, Man, and Cybernetics, Part C (Applications and Reviews), 42(6), 994-1002.

[13] H. Saadat, *Power System Analysis* McGraw-Hill Series in Electrical and Computer Engineering, 1999.

[14] H. Bervani, ‘*Robust Power System Frequency Control’*. 2th edition, New York Springer Verlag, 2014

[15] Nitesh Thapa, Nilu Murmu, Aditya Narayan, Birju Besra (2017). *Automatic voltage regulator and automatic loadfrequency control intwo-areapower system*. international Journal of Research in Engineering, Technology and Science. 1-7p

[16] P. Kundur, Power System Stability and Control. MacGraw-Hill, New York 1994.

[17] Shiroei, M., Toulabi, M. R., & Ranjbar, A. M. (2013). *Robust multivariable predictive based load frequency control considering generation rate constraint*. *International Journal of Electrical Power & Energy Systems*, *46*, 405-413.

[18] H. Bevrani, T. Hiyama, *Intelligent Automatic Generation Control*. ISBN -13: 978-1-4398-4954-5 (Ebook-PDF).

[19] Francis, R., & Chidambaram, I. A. (2012). *Control performance standard based load frequency control of a two area reheat interconnected power system considering governor dead band nonlinearity using fuzzy neural network*. *International Journal of Computer Applications*, *46*(15), 41-48

[20] Bevrani, H., Ghosh, A., & Ledwich, G. (2010). Renewable Energy Sources and frequency regulation: survey and new perspectives. *IET Renewable Power Generation*, *4*(5), 438-457.

[21] Sanki, P., Basu, M., & Pal, P. S. (2018, March). Study of AGC as two area thermal interconnected power system consisting WPG and SPG. In *2018 Emerging Trends in Electronic Devices and Computational Techniques (EDCT)* (pp. 1-6). IEEE

[22] Singh, V. P., Mohanty, S. R., Kishor, N., & Ray, P. K. (2013). Robust H-infinity load frequency control in hybrid distributed generation system. *International journal of electrical power & energy systems*, *46*, 294-305.

[23] Hayerikhiyavi, M., & Dimitrovski, A. (2021, April). A practical assessment of the power grid inertia constant using PMUs. In *2020 52nd North American Power Symposium (NAPS)* (pp. 1-5). IEEE

[24] Audu, N. A., Alphaeus, O., & Adamu, T. (2018). Effect of inertia constant on generator frequency and rotor angle. *Eng. Appl. Sci*, *3*(1), 6.

[25] Tamrakar, U., Shrestha, D., Maharjan, M., Bhattarai, B. P., Hansen, T. M., & Tonkoski, R. (2017). Virtual inertia: Current trends and future directions. *Applied Sciences*, *7*(7), 654

[26] Kerdphol, T., Watanabe, M., Hongesombut, K., & Mitani, Y. (2019). Self-adaptive virtual inertia control-based fuzzy logic to improve frequency stability of microgrid with high renewable penetration. IEEE Access, 7, 76071-76083

[27] Skiparev, V., Machlev, R., Chowdhury, N. R., Levron, Y., Petlenkov, E., & Belikov, J. (2021). Virtual inertia control methods in islanded microgrids. *Energies*, *14*(6), 1562

[28] K. Ang, G. Chong, "PID Control System Analysis, Design, and Technology," IEEE Transactions On Control System Technology, Vol. 13, No. 4, July 2005

[29] A. HALMOUS, H. ABBOU. "Flexible AC Transmission System based Automatic Generation Control, " Master thesis, University of Amar Telidji, Laghouat 2020

[30] M. Pant, “Particle Swarm Optimization, Department of Applied Science and Engineering,” Saharanpur Campus of IIT Roorkee. 2009

[31] X. Yang. Nature Inspired Metaheuristic Algorithms. 2nd Edition, Luniver Press, 2010

[32] Gavrilas, M. (2010). Heuristic and metaheuristic optimization techniques with application to power systems. *Technical University of Iasi, D. Mangeron Blvd., Iasi, Romania*.

[33] N. Sadhasivam, “Certain Investigation on Improved PSO Algorithm for Workflow Scheduling in Cloud Computing Environment”, Humburg, Anchor Academic Publishing 2017

[34] Nasiri, J., & Khiyabani, F. M. (2018). A whale optimization algorithm (WOA) approach for clustering. *Cogent Mathematics & Statistics*, *5*(1), 1483565

[35] Hasanien, H. M. (2018). Whale optimisation algorithm for automatic generation control of interconnected modern power systems including Renewable Energy Sources. *IET Generation, Transmission & Distribution*, *12*(3), 607-614

[36] Mirjalili, S., & Lewis, A. (2016). The whale optimization algorithm. *Advances in engineering software*, *95*, 51-67

Appendix

- **Two areas reheat thermal**

  Nominal parameters of the system investigated are:

Parameters	Area-1	Area-2
Frequency bias factor, Bi (p.u.MW/Hz)	0.3483	0.3827
Governor time constant, Tg (s)	0.08	0.06
Turbine time constant, Tt (s)	0.4	0.44
Droop constant, R (Hz/p.u.MW)	3	2.73
System inertia constant, H (p.u.MW s)	0.083	0.1010
Damping coefficient, D (p.u.MW/Hz)	0.015	0.016
Virtual inertia time constant, TVI (s)	10	10
Solar system time constant, TPV (s)	1.3	-
Wind turbine time constant, TWT (s)	-	1.5
Maximum limit of valve gate, VU (p.u.MW)	0.5	0.5
Minimum limit of valve gate, VL (p.u.MW)	-0.5	-0.5
Synchronizing coefficient, T12 (p.u.MW/Hz)	0.08	
Area capacity ratio between two areas, *a*12	-0.6	

- **Nonlinearities**

In this study, the GRC and GDB limits taken into account are given below: GRC = ± 12%

p.u. MW/min, GDB = ± 0.5 p.u. MW

- **The WOA settings**

Number of search agents N = 40

Maximum number of iterations T= 100